Report

Characterization of Alpha Radiation Hazards

Research and Development

153-121110-REPT-080
Revision 0

2016 April   avril 2016

UNRESTRICTED   ILLIMITÉE

© Canadian Nuclear   © Laboratoires Nucléaires
Laboratories   Canadiens

286 Plant Road   286, rue Plant
Chalk River, Ontario   Chalk River (Ontario)
Canada K0J 1J0   Canada K0J 1J0

Report

Characterization of Alpha Radiation Hazards

Research and Development

153-121110-REPT-080
Revision 0

Prepared by Rédigé par	_____ Candice Didychuk Radiobiology & Health
Reviewed by Examiné par	_____ Sheila Kramer-Tremblay Radiobiology & Health
Approved by Approuvé par	_____ Sheila Kramer-Tremblay (Acting Manager) Radiobiology & Health

2016 April

avril 2016

UNRESTRICTED

ILLIMITÉE

CW-511300-FM-168 Rev. 2

Ref. Procedure CW-511300-PRO-161

Document No. / Numéro de document:	153	121110	REPT	080
	Doc. Collection ID ID de la collection de doc.	SI Répertoire du sujet	Section	Serial No. N° de série

Document Details / Détails sur le document

Title
Titre

Characterization of Alpha Radiation Hazards

Total no. of pages
N^{bre} total de pages

70

For Release Information, refer to the Document Transmittal Sheet accompanying this document. / Pour des renseignements portant sur la diffusion, consultez la feuille de transmission de documents ci-jointe.

Revision History / Liste de révisions

No./N°	Date (yyyy/mm/dd)	Details of Rev. / Détails de la rév.	Prepared by Rédigé par	Reviewed by Examiné par	Approved by Approuvé par
	Revision / Révision				
0	2016/04/27	Issued as "Approved for Use"	C. Didychuk	S. Kramer-Tremblay	S. Kramer-Tremblay

TABLE OF CONTENTS

TABLES

TABLE OF CONTENTS

FIGURES

TABLE OF CONTENTS

TABLE OF CONTENTS

APPENDICES

1.   TASK OUTLINE

Table 1 Tasks

TASK	DESCRIPTION
1	Review and compile published data on the biosolubility of actinoids.
2	Recover mechanically collected, un-sized particles of irradiated UO_2, ThO_2, ZrO_2 and Fe_3O_4. Use sedimentation techniques to collect respirable particles with comparable hydrodynamic (aerodynamic) diameter as existing un-irradiated UO_2 particles held by the Radiological Protection Research and Instrumentation Branch at AECL, CRL.
3	Characterize actinoids and fission products present in irradiated samples (UO_2 fuel, ZrO_2 and Fe_3O_4) and concentrations.
4	Measure: (1) the *in vitro* (i.e., simulated lung fluid solubility methods and Tessier chemical extractions), (2) *in vivo* (i.e., instillation into rats) solubility of the materials and (3) the dissolution rate of un-irradiated UO_2 particles to serve as a standard reference. Use inductively coupled plasma mass spectrometry (ICP-MS) for analyses.
5	Measure the differential dissolution rates of major and minor radionuclides (Pu, Am and Cm isotopes, Sr-90 and Cs-137) from experimental particles using either mass spectrometry or radiochemical methods.
6	Analyze data to answer the following questions: Does the solubility of fuel change as a function of burn-up in the reactor? Do all radionuclides leach from particles at the same rate? How soluble are radionuclide contaminated ZrO_2 and Fe_3O_4 residues compared with un-irradiated UO_2? What is the appropriate inhalation solubility class, as defined in ICRP Publication No. 66?

2. DELIVERABLE OUTLINE

Table 2 Deliverables

Deliverable	Due Date	Update
Progress Report #1	2011/12-March-31	complete
Progress Report #2	2012/13-February-28	complete
Progress Report #3	2013/14-March-31	complete
Progress Report #4	2014/15-March-31	complete
Final Report	March 2016	

3.   GENERAL BACKGROUND

During the handling of nuclear fuel, reprocessing of radioactive wastes and general reactor maintenance at nuclear generating stations, there is a potential for the release and subsequent inhalation of irradiated fuel debris containing alpha-emitting radionuclides. At Bruce Nuclear Generating Station (NGS) Unit 1, for example, a problem was encountered when feeder pipe ends were being prepared in order to weld on new spool pieces. One of the specific tasks, referred to as "J-prep", consisted of removing the magnetite layer from the inner and outer surfaces of cut ends of feeder tubes in order to produce a clean surface available for the welding of replacement piping [1]. The task resulted in worker inhalation exposures to alpha-emitting radionuclides. In such an incident, where intakes such as this has occurred, the major isotopes contributing to dose have been higher actinides (i.e., plutonium (Pu), americium (Am) and curium (Cm)), which in terms of mass are inconsequential components of the inhaled material. Currently, bioassay methods based on urine for these higher actinides are either insufficiently sensitive to determine intakes at levels corresponding to dose limits or require specialized techniques such as accelerated mass spectrometry (AMS). Therefore, dose calculations are made by measuring a major component (i.e., Pu-239) in excreta followed by employing a reference hazard to estimate the dose to the worker from the higher actinides. This practice is justified, but only if all components within the inhaled material are leached from the particles at the same rate. This, however, has not been established for many materials that are known to contain a range of alpha- emitting radionuclides. Furthermore, following an inhalation exposure to such a material, the "worse-case" default calculations that are initially applied, commonly assume that the inhaled material is defined by the same solubility behavior (i.e., rate of dissolution) as insoluble fuel particles (i.e., uranium dioxide). Subsequent dose calculations are adjusted based on bioassay urine and feces ratios to more accurately reflect the solubility of the material. There is significant uncertainty regarding the form and solubility of these inhaled alpha-emitting materials and whether they are comparable to the reference insoluble fuel particles. For example, the inhalation exposure incident at Bruce NGS suggested a lung solubility of a 'moderately' soluble type M material by comparison to un-irradiated UO_2 fuel, which is classified by the International Commission on Radiological Protection (ICRP) as an insoluble type S material[2].

As the dose received by an individual is a function of the solubility of the inhaled material, this work was undertaken to better understand the chemical and biological solubility of un-irradiated UO_2 CANDU fuel particles and other actinide-contaminated materials, including thorium dioxide (ThO_2) fuel, irradiated-magnetite (Fe_3O_4) feeder pipe debris and irradiated UO_2 CANDU fuel. Due to the inability of most facilities (domestic and internationally) to obtain such materials or conduct further research on radioactive material, minimal information is available concerning the lung solubility of irradiated reactor debris. Therefore, no experimental biosolubility data is available to estimate the dissolution rate of these materials following internal contamination of the lungs. This study directly assesses the solubility of these alpha-contaminated materials collected from Canadian NGS's and of un-irradiated UO_2 CANDU fuel and ThO_2 fuel obtained from local fuel fabrication facilities (Canadian Nuclear Laboratories (CNL), Chalk River).

The results obtained from this work will facilitate the improvement of the assessment of radiological hazards that are present during work on or in association with CANDU nuclear reactors and provide a better base for the initial estimate of dose following worker intakes of irradiated debris. This is of value to our radiation protection programs when in urgent need of assessing dose and the appropriate bioassay schedule for worker bio-monitoring. The information will also be used to estimate the appropriate ICRP inhalation classification [i.e., F (soluble), M (moderately soluble) or S (insoluble)] for the materials.

4.   MATERIAL CHARACTERIZATION

All materials for the project have been identified and obtained. The samples include UO_2, ThO_2 and irradiated UO_2 fuel at 5 different burn ups, and actinide contaminated ZrO_2 and Fe_3O_4 residues from reactor pressure tubes and feeder pipes, respectively. The irradiated UO_2 fuel and ZrO_2 were obtained from the Pickering Nuclear Generating Station (PNGS) and the Fe_3O_4 from the Gentilly-2 Nuclear Generating Station (G-2-NGS). The UO_2, ThO_2 and Fe_3O_4 debris, and all 5 irradiated UO_2 fuel samples, have been processed to obtain particles with an aerodynamic diameter of 1-5 µm. Currently, the ZrO_2 debris is stored as a dry powder and will be sized when needed for experimentation. As the size sedimentation procedure is conducted in a water column, all samples remain stored in water until use. As the procedure is brief, size sedimentation is best performed on an as-required basis.

The materials identified and collected are discussed below.

4.1   Un-irradiated UO_2 fuel

Natural uranium dioxide (UO_2) milled powder was collected from the Fuel Development Facility located at CNL, Chalk River. Natural UO_2 consists primarily of U-238 (~99.28%) with a half-life of 4.468 billion years which alpha decays (4.267 MeV) to Th-234. Uranium, as the UO_2^{2+} uranyl ion, behaves chemically similar to calcium (Ca) and is transferred through the body in a similar manner. There is a significant amount of literature on the biological properties and bio-monitoring of uranium oxide compounds, including UO_2. Although well documented, the literature also indicates that UO_2 fuel produced at different fuel development facilities can behave differently with respect to its solubility depending on the fabrication or processing history [3]. Therefore, it is encouraged to gather location-specific solubility data on the fuel [4, 5]. Following inhalation, UO_2 particles have been identified in the literature to demonstrate an average long-term lung retention $T_{1/2}$ of 600 d. Once the uranium species dissolve and absorb into the blood stream, the largest fractions tend to deposit in bone and kidneys. As experimentally derived absorption rates of uranium to blood and target organs following inhalation using a rat model have been deemed relatable to that in humans, and as the biological solubility and absorption rates are frequently being reviewed by the ICRP, uranium was chosen as a comparator for the other materials tested in this study [6, 7].

4.2   Thorium Dioxide (ThO_2)

The CANDU® reactor system can effectively use thorium oxide fuels, which have become a fundamental part of the fuel cycle vision for the reactor. At CNL, Chalk River, experimental mixed oxide (MOX) fuel containing ThO_2 as Th-232 has been irradiated and has undergone post-irradiation examination (PIE) to evaluate its performance. Since thorium-based fuels are under consideration for use in CANDU® reactors, and due to the gap in information regarding its biological solubility and biokinetics, determining the lung solubility of ThO_2 is necessary for improved radiological assessment and protection requirements [8]. This information is also needed by CNL for dose assessment purposes for staff performing work in fuel development.

For this study, thorium dioxide (ThO_2 as Th-232), a white crystalline milled powder, was obtained from the Fuel Development Branch, CNL. Thorium-232 has an exceptionally long

half-life of ~1.41 x10^{10} years and decays through a number of daughter radionuclides by alpha (α), beta (β) and gamma (γ) emissions to the stable nuclide Pb-208. Due to its physical characteristics as an α-emitter and its assumed biokinetic behaviour following incorporation in the human body (its decay chain remains at the site of deposition, i.e., the lungs), Th-232 is considered one of the most radio-toxic actinides per unit activity (Bq) [9, 10].

4.3   Irradiated UO$_2$ fuel

Currently, there is neither experimental data nor information available to assess the dosimetric consequences following internal exposure to this material. In the event of internal contamination via inhalation, solubility classification and dose calculations are determined based on many of the characteristics and data that are available for un-irradiated UO$_2$ fuel. Irradiation of UO$_2$ fuel not only affects the physical state of the fuel from restructuring processes, but also its chemistry. There is the production of an array of actinides and fission products, an increase in fuel porosity, formation of fractures, gaps and production of gases [2]. Figure 1 illustrates some of these changes, all of which could significantly affect the solubility of the material and are suggestive of a fate different than that of un-irradiated fuel, if internalized.
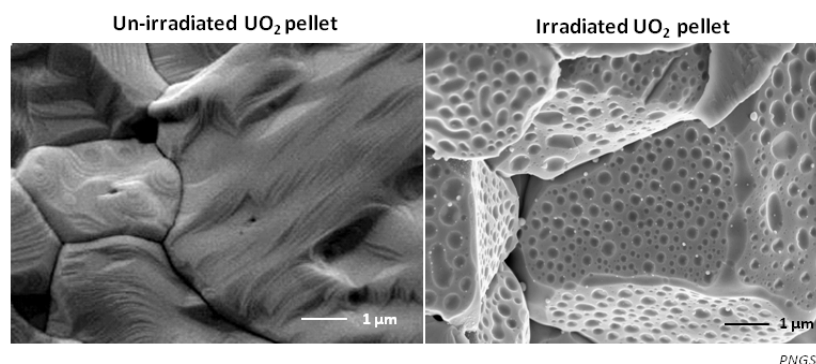
Figure 1 Scanning electron micrographs showing the physical effects of irradiation on UO$_2$ fuel at high burn-up.

Table 1 Irradiated UO$_2$ fuel samples obtained from Pickering Nuclear Generating Station.

Fuel IDs	Insertion Date	Discharge Date	Residency Time (d)	Discharge Bundle Burnup* (MWh/kgU)	Max Bundle Power (kW)
2009 PNGS-A FUEL					
M73397Z	2005/07/29	2007/03/03	582	274	588
N71589C	2006/03/25	2008/04/28	765	187	598
N75450C	2006/05/26	2008/03/21	665	171	600
2007 PNGS-B FUEL					

| N40589C | 2004/01/30 | 2005/01/12 | 348 | 157 | 595 |
| N58817C | 2005/08/15 | 2007/03/22 | 584 | 224 | 546 |

Burn up is a term used for the total energy produced by a nuclear fuel per unit mass. Typical units: MWd·Kg^{-1}U.

The actinide and fission products present in the irradiated UO_2 fuel samples were estimated using CNL code data ('WOBI': WIMS-ORIGEN Burn-up Integration-version 2.3.0), which is used to predict the composition of cooled CANDU® fuel (Reactor Physics Branch, CNL). The actinides and major fission products for the irradiated UO_2 fuel samples have been estimated. For each fuel ID, the radionuclide specific activity (Ci·kg^{-1}) was assessed for 1300-2500 d of cooling, dependent on the time between reactor discharge and a sampling date of February 1, 2012. Also, for each fuel component, the activity data were analyzed by first eliminating all radionuclides not contributing at least 0.1% to the total activity.

4.4　　　　　Pressure Tube (ZrO_2) sample:

The pressure tube oxide samples were taken at approximately 3.7 m from the inlet end of the tube (Pressure tube ID: P6M14-J). Figure 2 shows the oxide surface on the interior body of the pressure tube. The tube was installed in 1979 and removed in 2007, with 162,230 EFPH (Equivalent Full Power Hours) and 169,510 HH (Hot Hours). At the sampling location, the neutron fluence was 1.25×10^{22} n/cm^2 and the average operating temperature was 277°C.

The oxide removal/collection was undertaken using a 20 grit boron carbide ball hone in the Universal hot cells at CNL. A small container was used to store the oxide debris collected. Figure 3 identifies the cut piece of pressure tube and the ball hone being used to grind the interior surface of the tube.
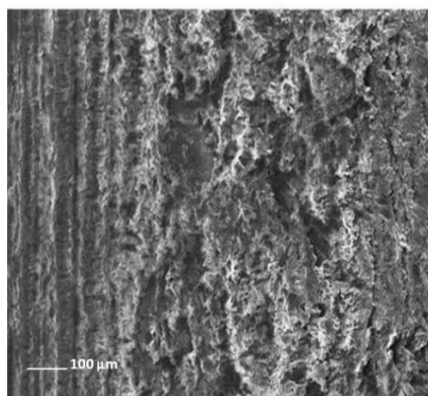
Figure 1 SEM image representing the interior oxide (ZrO_2) layer of the post-service pressure tube.
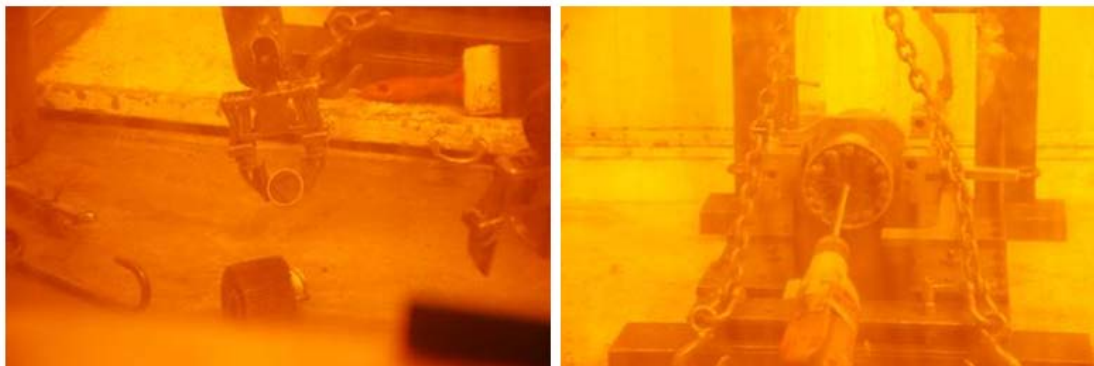
Figure 2 Collection of the contaminated ZrO2 material from the interior surface of a cut piece of a pressure tube.

4.5   Feeder Pipe (Fe$_3$O$_4$) sample:

Scrapings from two 'as-received' feeder pipe specimens (G-11-13 and G-11-14) were obtained from the Component Life Technology Branch at CNL for this study. These specimens are identified in Figure 4. Scrapings from the two samples identified were combined to provide a total weight of 180 mg, which was used for analysis. Note that the inlet feeder pipe was removed in 2006 and most short-lived radionuclides had decayed by the date of the measurements in Table 2. The pipe was received by CNL in 2008 and analyzed in 2011.

Figure 3 Feeder pipe specimens

The known total weight of the sample was dissolved, and converted to a known weight and volume in 2M nitric acid. The gamma (γ)-emitting radionuclides were determined by counting a known aliquot of the solution along with corresponding blanks for 8 h. A known amount of the dissolved sample was also used to prepare sources for the measurement of gross alpha (α) and gross (β) activities. The sources were counted on an optimized gas-flow proportional counter (GPC). The reported gross α and gross β activities were based on count durations of 4 h and 2 h, respectively, and can be found in Table 4.

A known aliquot of the sample was then spiked with a specific concentration of tracer for chemical recovery analysis. The sample was processed through a co-precipitation procedure for the removal of excess iron, as it is a magnetite-based sample, prior to the separation of americium (Am), curium (Cm), and plutonium (Pu) isotopes by radiochemical methods. The separated actinide isotopes were electroplated onto stainless steel discs for alpha spectrometry. Table 4 indicates the resulting activity

Table 2 Estimated activity concentrations (Bq/g of dry deposit) of the actinide isotopes and the gamma- emitting radionuclides in the deposits from Gentilly-2 Feeder Pipe specimens (year of analysis 2011).

Sample ID	Actinide	Bq/g *of dry sample*
Scraping from Feeder Pipe specimen G11-13 and G11-14	Am-241	128 ± 5
	Cm-243/244	570 ± 20
	Pu-238	24 ± 2
	Pu-239/240	132 ± 6
Gross α activity: (8.5 ± 0.3) x 10^2	γ-emitting radionuclides	
	Mn-54	$(8 \pm 3) \times 10^2$
	Co-60	$(1.3 \pm 0.1) \times 10^6$
Gross β/γ activity: (1.3 ± 0.02) x 10^6	Nb-94	$(4.0 \pm 0.5) \times 10^3$
	Sb-125	$(3.2 \pm 0.6) \times 10^3$
	Cs-137	$(4 \pm 2) \times 10^2$

A more comprehensive radiochemical analysis will be conducted on this sample. As the material is now of the proper size range for use in this study (1-5 µm; AMAD), the actinides and gamma-emitting radionuclides will be re-characterized, including measurement of ^{90}Sr and ^{55}Fe, using methods discussed in this report.

Noteworthy is that the specific activity of this material is quite low. It would seem impossible to intake an ALI, as >1 gram of the debris would have to be inhaled.

5.   SIZE SEDIMENTATION & CHARACTERIZATION OF MATERIALS

Deposition of an inhaled particulate throughout the respiratory tract is a function of the particulate's size, more specifically its aerodynamic diameter (AMAD). Occupational exposures are assumed to be from 5 µm AMAD aerosols; therefore, particulate aerodynamic diameter is assumed to be log-normally distributed with a geometric mean of 5 µm and a geometric standard deviation of 2.47 (ICRP 66). The aerodynamic particle diameter is the diameter observed due to irregularities in shape and is used in the determination of aerodynamic deposition.   In the event of an occupational exposure where the size of the inhaled radionuclide-contaminated material is unknown, the ICRP recommendation is to predict an individual dose based on using the default assumption that 5 µm (AMAD) particles were inhaled by the individual. This is a result of particles 1-5 µm (AMAD) proving to have an intake efficiency of 1, meaning an inhalability of 100%.

All materials were fractioned such that each is of a similar size (1-5 µm, AMAD). To obtain samples of a similar particle size distribution, the settling velocity (V_t) of the particles in a water column was determined by applying Stoke's equation:

$$V_t = \frac{gd^2(\rho_p - \rho_m)}{18\mu}$$

where (g) is the effect of gravity, (d) is the particle diameter, ρ_p and ρ_m are the mass density of the particle and of the medium, respectively, and (μ) is the viscosity of the medium.

This allowed for the particle diameter in each sample to be controlled. This method was initially applied to un-irradiated UO_2 and ThO_2 particle samples. The size separation method involved two steps as shown in Figure 5. Step one involved settling of the size fraction ≥ 5 µm. This is related to a settling a velocity of 49.1 cm/h for un-irradiated UO_2 and 44.2 cm/h for ThO_2. Therefore, for a suspension height of 10 cm for each sample in a column, durations of 0.2 h and 0.23 h are required to settle out the fractions of un-irradiated UO_2 and ThO_2 that are ≥ 5 µm. The fractions remaining in suspension were then collected and used to perform the second separations. During this step, settling velocities corresponding to 1 µm particles were calculated. For un-irradiated UO_2 and ThO_2, this corresponds to a settling time of 5.1 h and 5.6 h, respectively. In this case, the settled fractions were collected for further experimental work in the study.
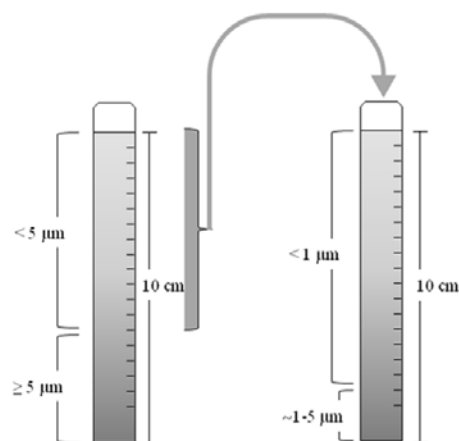
Figure 4 Size separation of the particulate using sedimentation rates in two water columns.

5.1   Un-irradiated UO$_2$

Figure 6 shows the results of the particle size distribution (PSD) curves collected using a Horiba LA-900 Laser Diffraction Analyzer (Fuel Development Branch, CNL) for the un-irradiated UO$_2$ particles before and following the size sedimentation process. The un-irradiated UO$_2$ particles were found to have a geometric mean diameter of 0.70 ± 0.51 µm, which translated to an aerodynamic diameter of 2.32 µm. The final concentration of the sized UO$_2$ particulate suspension was 3.25 ± 0.09 mg·mL^{-1}.
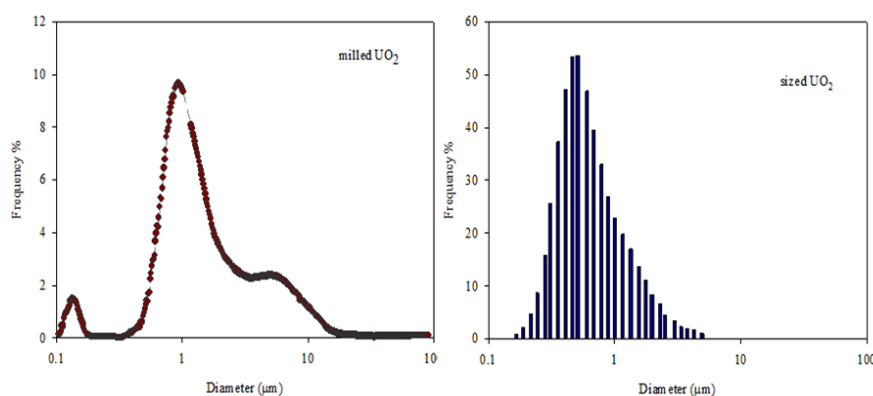
Figure 5 Particle size distribution curves of milled and sized un-irradiated UO2 particles.

Note that there are several ways to measure the 'size' of a particle, which may give differing results for the same particulate. Commonly, the results are reported in terms of an 'equivalent' sphere. For this study, the aerodynamic diameter was calculated from the geometric diameter (d) according to the equation below, where ρ_p and ρ_m correspond to the density of the particulate (UO$_2$) and the medium (water), respectively. Figure 7 provides an example of the scanning electron microscopy (SEM) image obtained for the sized un-irradiated UO$_2$ particles.

$$d' = \left(\sqrt{(\rho_p/\rho_m)} \right) \times d$$
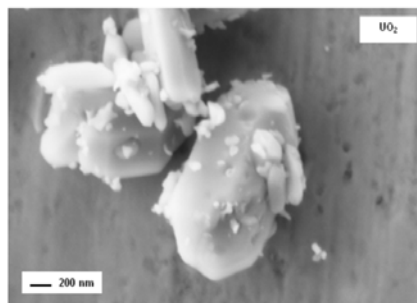
Figure 6 An SEM image of sized UO2 particulates.

5.2   ThO$_2$ Sample

For ThO$_2$, following the size sedimentation process, the resulting particles averaged a geometric diameter of 0.71 ± 0.59 µm, as shown in Figure 8. This value translated to an average aerodynamic diameter of 2.25 µm. A representative SEM image for the ThO$_2$ particles obtained is shown in Figure 9. The final concentration of the sized ThO$_2$ fuel particulate suspension was 3.15 ± 0.09 mg·mL^{-1}.
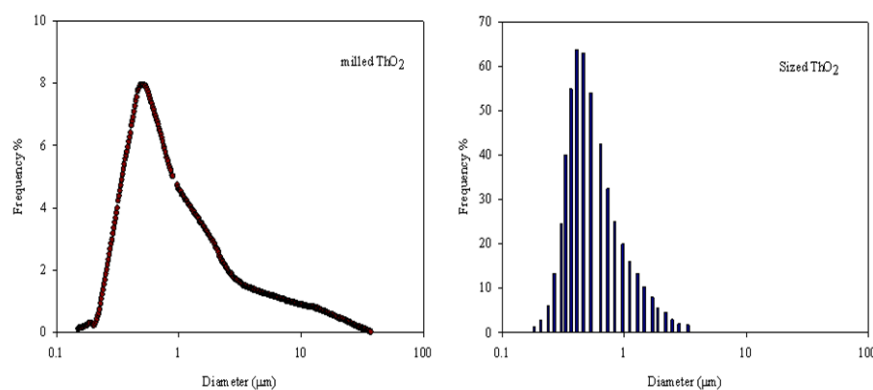
Figure 7 Particle size distribution curves of milled and sized un-irradiated ThO2 particles.
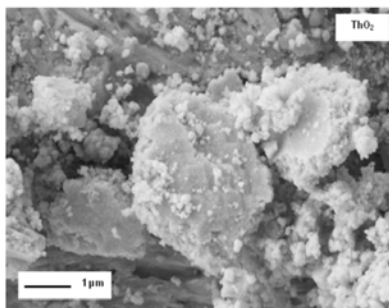
Figure 8 SEM image of sized ThO2 powder.

The results for the un-irradiated UO_2 and ThO_2 particulate demonstrated that using Stokes equation to calculate the settling rate of these materials in a water column to obtain particles of a specific size range is a fast, considerably accurate and effective method that can be used to provide particles of different materials of a comparable size.

5.3   Irradiated UO_2 Fuel

The size sedimentation method was also applied to the irradiated UO_2 fuel samples using the same parameters for determining the appropriate size setting velocities identified for un-irradiated UO_2 fuel. However, due to the Horiba LA-900 Laser Diffraction Analyzer no longer being operable, PSD curves for the sized irradiated fuel samples are unavailable. As the method has proven to produce reliable and consistent results for other materials for which it was applied, there is confidence that the irradiated UO_2 fuel particle sizes will be similar to those obtained for UO_2 and ThO_2, and are therefore comparable.

However, efforts have and will continue to be made for the purchase of a new Horiba LA-960 Laser Diffraction Particle Size Analyzer, as its role in particle characterization and dosimetry is of considerable value.

5.4   Radiochemical Analysis of Respirable Sized Irradiated UO_2 Fuel

Although the activity concentration (MBq/g) for both the actinides and fission products were predicted using CNL code data, further analyses were required following the size sedimentation of the irradiated fuel samples. The final activity concentrations in the samples were re-evaluated using radiochemical separation and analysis techniques. This provided experimental data on the fuel samples that could be compared with values derived using fuel codes.

A sequential radiochemical separation procedure, as shown by the schematic in Figure 10, was adapted for the analysis of the actinide isotopes as well as radio-strontium (^{90}Sr) present in the samples. Figure 11 shows the 4-cartridge separation of the irradiated fuel samples, where the samples were passed through a series of pre-conditioned anion exchange and extraction chromatography columns for the separation of Pu, U, Am/Cm and [90]Sr. Briefly, an aliquot of irradiated UO_2 fuel suspension was obtained, to which appropriate tracers, including [243]Am, [233]U, [242]Pu and stable Sr, were added for correction of any loss of chemical recovery. The

samples were then dissolved under highly acidic conditions, evaporated to near dryness and re-suspended in an 8M HNO_3 solution. After the addition of a small amount of $NaNO_2$ for valancy adjustment of actinides, the samples were passed through a series of pre-conditioned anion exchange [AGMP-1M resin (Bio-Rad Laboratories Canada Ltd., Mississauga ON)] and extraction chromatography columns (Eichrom UTEVA, DGA and Sr resins; Eichrom Technologies, Inc., Illinois, USA), for the separation of Pu, U, Am/Cm and ^{90}Sr. The columns were rinsed with 8M HNO_3 and split for elution.
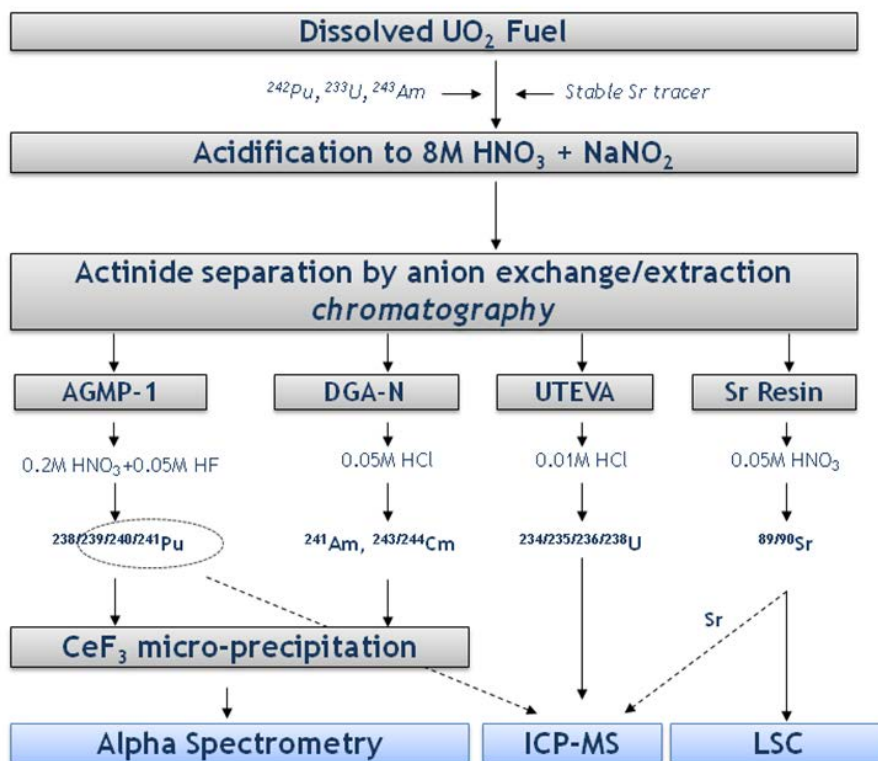
Figure 9 Schematic representation of the radiochemical separation procedure for characterization of irradiated UO$_2$ fuel.

Figure 10 Four column radiochemical separation of actinides and Sr-90.

Per irradiated fuel sample analyzed, a total of 4 eluate samples (i.e., Pu, U, Am/Cm and Sr) were obtained. The U eluate and half of the Pu eluate were sent to the CNL Analytical Chemistry Laboratory for ICP-MS analysis of the U and Pu isotopes, specifically, $^{238, 236, 235, 234}$U and $^{241, 240, 239}$Pu.

All of the Am/Cm Eluate and the other half of the Pu eluate were followed with CeF_3 micro-precipitation and filtered onto 0.1 µm Resolve™ filters (Eichrom Technologies, Inc.) to prepare thin layer sources for alpha spectrometry. The samples were counted for 16 h using an Octête Plus® Alpha Spectrometry Workstation (AMETEK/ORTEC Inc., Oakridge, Tennessee, USA). The activity concentrations of ^{241}Am, ^{242}Cm, $^{243/244}$Cm (the combined activities of both ^{243}Cm and ^{244}Cm, as their spectral lines overlap in the alpha spectrum and cannot be separated), ^{238}Pu and $^{239/240}$Pu (the combined activities of both ^{239}Pu and ^{240}Pu, as their spectral lines overlap in the alpha spectrum) isotopes are reported.

For the ^{90}Sr eluate, a small fraction of the sample was diluted in 0.1M HNO_3 and sent to Analytical Chemistry at CNL for analysis of the stable Sr tracer by ICP-MS. The remainder of the Sr eluate was mixed with Ultima Gold AB liquid scintillation (LS) cocktail for counting on a Hidex 300SL liquid scintillation counter immediately following the chemical separation.

Gamma spectrometric analysis was carried out using a coaxial high purity germanium (HPGe) detector with lead shielding (AMETEK/ORTEC). The detection efficiency was calibrated with a multi-gamma source standard. The sample was counted for 4 hours.

5.4.1   Results

Figures 12 – 17 of this technical note represent the radio-chemically measured and code-derived values for the percent mass (g/kg $_{uranium}$), activity (Bq) and dose (Sv) contributions for the extensive number of actinides and fission products present per fuel ID (all 5 samples), as listed in Table 3. The 50 year committed effective dose (CED) contributions were determined by multiplying the corresponding inhalation dose coefficients by the activity of each measured isotope. Appropriate dose parameters, such as solubility and particle size (5 μm; AMAD), were selected for each radionuclide based on ICRP 68 recommendations for occupational exposure. The dose coefficients used for the dose calculation were those published in ICRP Publication 68.

Also, in order to evaluate the relative contribution of different radionuclides to the CED, an assumption was made that the intake by inhalation is equivalent to the activity of material collected and present per fuel stock created, although such an intake is unlikely.

All activities were decay-corrected to the sampling date (February 1, 2012). Also, since the alpha spectral lines of Cm-243/244 overlap each other, the two Cm isotopes could not be separately identified by alpha spectrometric analysis. However, it is expected that Cm-244 will dominate the combined activity for these two Cm isotopes, as a simulation using high fuel burn-up models predicted that Cm-244 would be more than 10 times as abundant as Cm-243 by activity. Therefore, the dose coefficient for Cm-244 (9.5×10^{-6} Sv/Bq) was used for the calculation of the combined dose from the two Cm isotopes.

Note that although the five irradiated fuel samples and their measured results using radiochemical analyses have been reported with the corresponding isotopic compositions from code derived values in Figures 12-17, this is not meant to be a validation effort. Rather, the two sets of data are meant to demonstrate the similarities in respect to isotopic components following a given burn up and cooling period and for an overall general comparison. This is due to the large uncertainty or difference in how the samples were each collected originally prior to analysis. Nevertheless, this information provides very useful information on the radionuclides present, activities and calculated dosimetry.
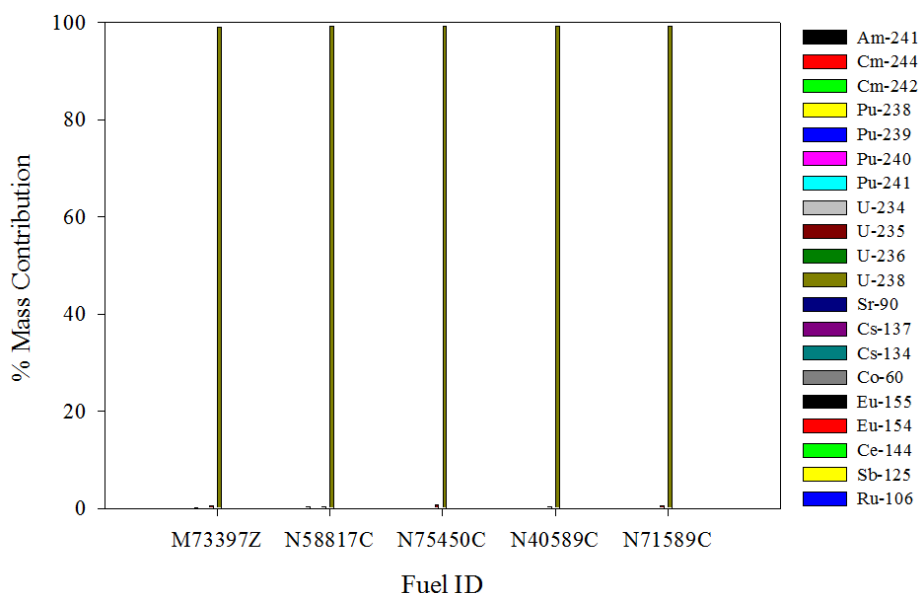
Figure 11 Percent Mass contribution of irradiated UO₂ associated radionuclides according to burn up Fuel ID.
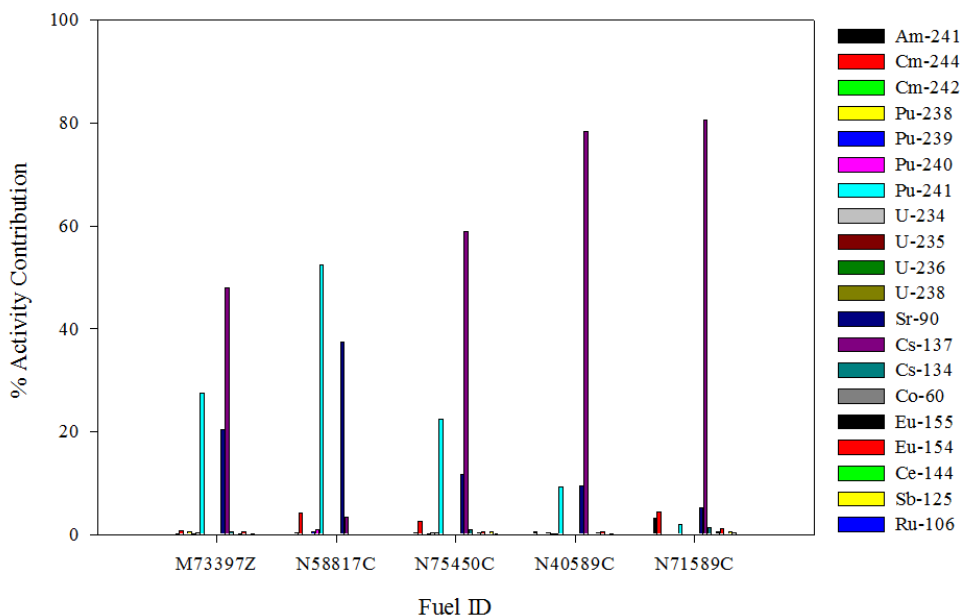
Figure 12 Percent activity contribution of irradiated UO₂ associated radionuclides according to burn up Fuel ID.
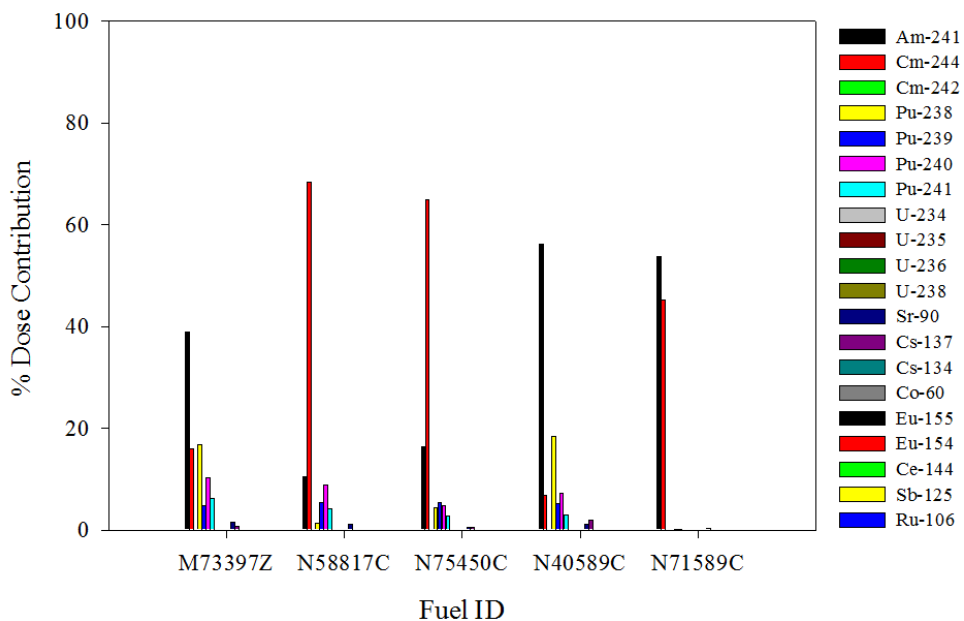
Figure 13 Percent dose contribution of irradiated UO₂ associated radionuclides according to burn up Fuel ID.
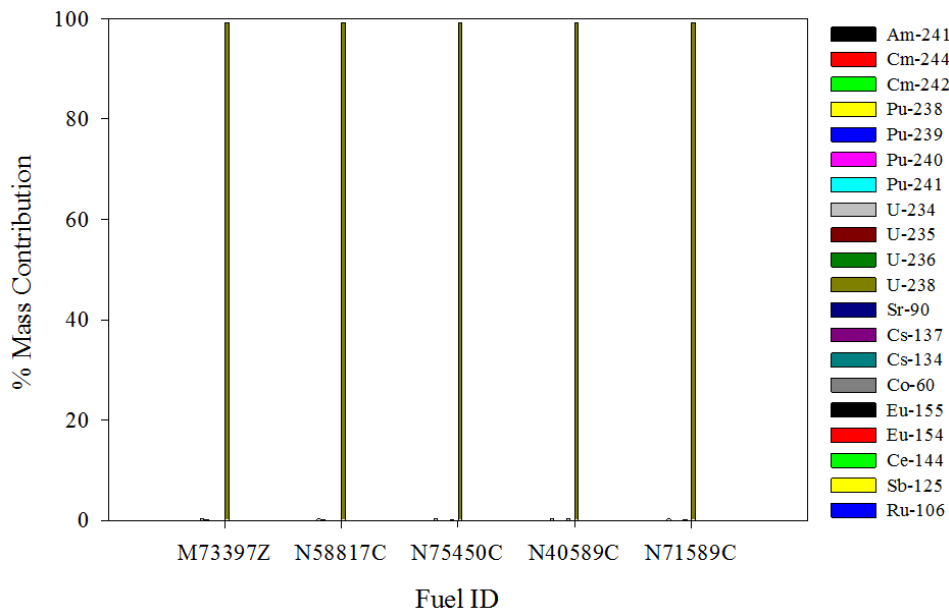
Figure 14 CODE DATA: Percent Mass contribution of irradiated UO$_2$ associated radionuclides according to burn up Fuel ID.
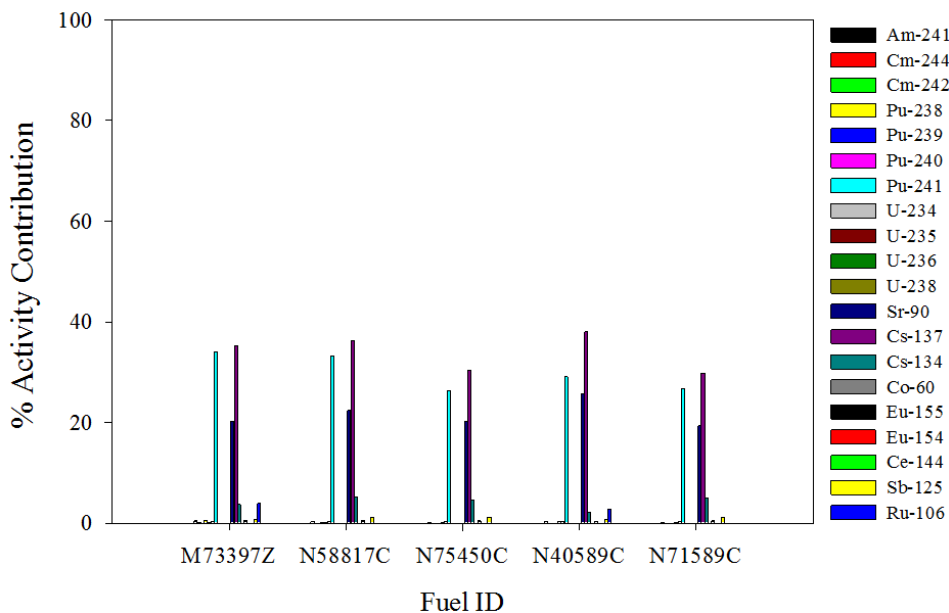
Figure 15 CODE DATA: Percent Activity contribution of irradiated UO$_2$ associated radionuclides according to burn up Fuel ID.
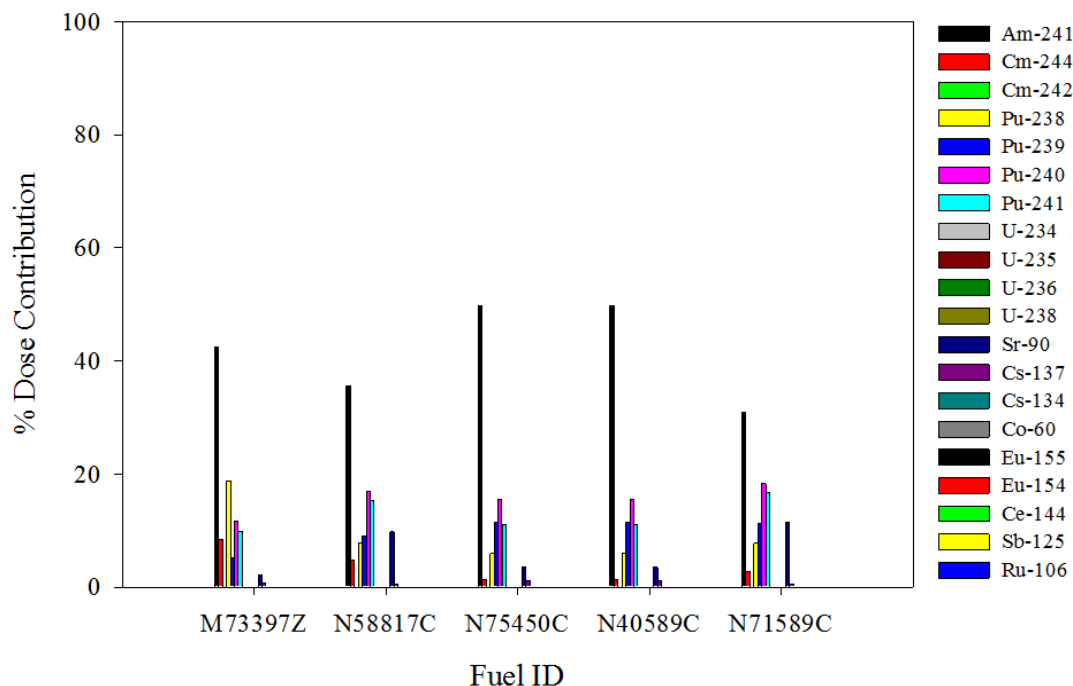
Figure 16 CODE DATA: Percent Dose contribution of irradiated UO₂ associated radionuclides according to burn up Fuel ID.

The dose contribution of the 5 irradiated fuel samples decreased with cooling of the fuel following its removal from the reactor, as short-lived and intermediate-lived fission products (and some fuel derived constituents; i.e., Cm-242, Np-239) decayed away. The contribution of fission products to the total dose from inhalation also decreased rapidly with cooling, such that the long-live alpha-emitting radionuclides dominated the predicted inhaled dose.

In Figures 12 and 15, it can be seen that U-238 is the main contributor to the bulk mass of the fuel with > 99% contribution in all 5 fuel ID's. Both measured and code analyses indicate Cs-137, Pu-241 and Sr-90 isotopes as having the highest percent activity contributions, respectively, shown in Figure 13 and 16. These isotopes accounted for more than 90% and as much as 98% of the total estimated activity that could be inhaled. The code data predictions for the Cs-137 and Pu-241 activity contributions were calculated to be similar to each other, for all burn ups identified. However, the measured samples demonstrated Cs-137 to be higher than the predicted values, in some cases as much as 50% greater, and the Pu-241 activities to be significantly lower.

With respect to the calculated CED, the alpha-emitting radionuclides contributed the highest estimated dose. The actinides accounted for more than 62% and as much as 85% of the estimated CED following an inhalation. A major alpha-dose contributor was Am-241 for all five fuel samples, which is also predicted by code data. Significant dose contributions were also observed from Pu-238, 239, 240 and 241, Sr-90 and notably Cm-244. The Cm-244 fractional CED contribution for the radio-chemically measured samples was significantly higher than

anticipated with respect to the values predicted using code data. This along with differences observed with activity contributions, could indicate the code data to be wrong.

Ideally, in order to detect a possible actinide intake, in this case as a result of an irradiated UO_2 fuel intake, a signature isotope should be used that is both a fission product of the fuel and has a long half-life such that it is detectable long after internalization. Cesium-137 (which decays to produce a strong gamma-emitter, Ba-137m), is commonly considered as a useful indicator for such a purpose and is proven ideal in this situation as well, as can be seen in the activity contributions reflected in the figures above.

6.   IN-VITRO SOLUBILITY METHODS

Dissolution plays a major role in inhalation toxicology and is significantly affected by the physical and chemical properties of the material, and as such, can be estimated by *in vitro* dissolution tests. Although *in vivo* data is preferred, *in vitro* experimental tests provide us with relative values, which allow avoidance of animal usage, meaning low cost and fast. *In vitro* methods are used as screening tools to estimate material solubility and possible ICRP classification for biokinetic and dosimetric modelling. *In vitro* tests can prove valuable in providing a first approximation of dissolution parameters and can be helpful in preliminary dosimetric calculations when no other information on a material is available.

6.1   Chemical Solubility Test: Sequential Extractions

6.1.1   Manuscript Draft

A manuscript has been drafted and approved for Publication on this topic.

The following section includes the draft manuscript, which incorporates both previous and new data, on using a sequential extraction method to characterize the solubility behaviour of un-irradiated UO_2, irradiated UO_2 and ThO_2 Fuel.

A Radionuclide Sequential Extraction Method to Evaluate the Solubility of Reactor Fuel Particulate

Candice Didychuk[1*], Sarah Frye[1], Kathryn Carson[2], Dominic Larivière[3], Nicholas Priest[1]

[1]*Canadian Nuclear Laboratories, Chalk River, Ontario. Canada, K0J 1J0*
[2]*Western University, Department of Microbiology & Immunology, London, Ontario. Canada, N6A 3K7*
[3]*Université Laval, Département de chimie, Québec City, Québec. Canada, G1V- 0A6*

Introduction

The different stages of the uranium nuclear fuel cycle including mining, milling, fuel conversion and enrichment, fuel fabrication, reactor operations, waste handling and storage, provide the opportunity for a radionuclide release, contamination of the environment and radiological risk to humans. Commonly, the areas surrounding the facilities associated with such activities become, to some extent, contaminated and present a possible hazard [1-4]. Monitoring the behavior of released contamination associated with these nuclear facilities is of significant concern to industry, regulators and the general public. To support radiation protection requirements, efforts are made to better understand the characteristic environmental and biological solubility of the radionuclide-contaminated materials that may be released by these facilities. Providing an indication of the amount of contamination that will become environmentally available and the conditions, under which incorporated radionuclides within a material matrix may be released is important for both pre-emptive and retrospective risk assessments. Despite increased research,

little information is available concerning the fate of many radionuclide-contaminated materials after they are released and the radiological hazard they may prevent. Preliminary characterization in terms of dissolution behaviour upon entry into the environment and under selected environmental conditions is required to provide critical insight on how to improve released-materials risk assessment. Such characterisation also provides a basis for a better understanding of the chemistry and the conditions under which fixed radionuclides may be released from fuel matrices. -

Uranium dioxide (UO_2) is used as a fuel for nuclear reactors, worldwide, in the form of sintered pellets. Although much information is documented regarding virgin UO_2 fuel solubility in a number of environmental settings (e.g., ground water, soils and vegetation), as well as for internalization in the body, reactor-irradiated UO_2 fuel (spent fuel) has received far less attention [5]. During reactor operation, the composition of the pure and modestly radioactive UO_2 fuel gradually changes as ^{235}U is fissioned to produce fission products and transuranium elements (neptunium, plutonium and other higher actinides). The latter form mostly through neutron capture by ^{238}U and subsequent beta (β) decay. With irradiation the UO_2 fuel becomes chemically complex and extremely radioactive[6]. When removed from the reactor, the radioactivity is a factor of a million times higher than that of fresh fuel. After one year, the dose rate at one meter from a fuel assembly is approximately 1 kGy·h^{-1}), i.e. enough to provide a lethal dose to man in less than one minute [7,5]. As irradiated fuel retains many of the transuranium elements and fission products within its structure, there is also an increase in fuel porosity with the formation of fractures, gaps and production of fission gases throughout [7]. he bulk of penetrating beta (β) and gamma (γ) ionizing radiation / activity results from the decay of fission products: principally cesium-137 (^{137}Cs), strontium-90 (^{90}Sr) and iodine-131 (^{131}I) and these may be relatively short-lived (<100 y). In terms of dose, the alpha-(α) emitting radionuclides produced (i.e., plutonium, americium, curium) are of particular concern to the environment and public health as they contribute significantly to dose, despite being inconsequential components of the irradiated UO_2 fuel (in terms of mass). These actinoids are highly radiotoxic and are long-lived with half-lives ranging from days up to millions of years[8,9]. Due to the gap in information surrounding the solubility of irradiated reactor fuel, it is commonly assumed that the dissolution behaviour of irradiated UO_2 either in the environment or if internalized, is similar to that of un-irradiated UO_2 fuel. It is also assumed that the actinide and fission products, produced within the fuel matrix, will leach from the fuel at the same rate and as a result of the bulk dissolution of ^{238}U. In contrast, for radiological protection dosimetry it is assumed that the various components behave independently with a solubility type classification that is element specific, e.g., solubility type F for caesium isotopes, and type S for plutonium isotopes etc. It is not known which of these assumptions is the most realistic and there is significant uncertainty regarding such assumptions which have yet to be thoroughly investigated. Nevertheless, there is evidence to suggest that the significant morphological and chemical changes observed in the UO_2 fuel following irradiation do result in solubility changes.

The environmental and biological availability of fuel radionuclides is a function of their physical and chemical form. Investigations have shown that sequential extraction / fractionation methods are widely used to produce information on solubility for characterization and radionuclide risk assessment, as they offer the ability to simulate some conditions encountered in the

environment[10-13]. Fractionation in sequential extractions involves the operationally defined selective dissolution of the radionuclide components within a solid phase material matrix, combined with measurements of the analyte radionuclides released during the dissolution reaction. The results of the method provide indirect evidence of the conditions under which radionuclides may be released from a matrix and their possible association within that material matrix. Of the methods that have been deployed the Tessier sequential extraction method, or variations of it, is the most commonly used to assess the mobility and availability of stable and radioactive elements under controlled conditions. This method allows the analyst to partition the particulate into individual sub-fractions, while performing either radiometric or elemental measurements on the analyte fractions [14]. The National Institute of Standards and Technologies (NIST) has adopted a modified Tessier approach as its standard method for the characterization of soil and sediment standard reference materials for radionuclide extractability [14-17]. The method incorporates five extraction steps designed to provide a different, and sequentially, more aggressive attack on the material. The method further provides a standardized means of obtaining information regarding the dissolution behavior of a material, leachability of individual radionuclides from the matrix and the mobility / availability of the radionuclides in the natural environment[17,15].

This study implements a modified NIST sequential extraction method to profile the general solubility properties of un-irradiated and irradiated UO_2 fuel particulates. These present a contamination and radiological hazard to both the environment and humans when they are released during fuel manufacture, normal reactor, reactor maintenance and fuel handling/storage operations[15]. Understanding how fuel, pre- and post-irradiation, may interact with local and rapidly changing environments is essential to better understand possible hazards in the event of a release [18,19]. The solubility of thorium dioxide (ThO_2) particulate was also investigated because it is an alternate nuclear fuel component and because there is currently an information gap concerning thorium solubility for radiation protection and dosimetry. This is so even though it is commonly assumed that this refractile oxide is insoluble under even the most aggressive conditions [20,21].

The level of characterization of reactor fuel achieved using sequential dissolution is a key when deducing the elution profiles of individual radionuclides and the identification of those that may have greater than average bioavailability. This information will highlight those radionuclides most likely to be released and migrate, under natural leaching, from the fuel matrix causing contamination in surrounding soils, vegetation and/or ground water. The objective of the study was to assess the utility of the Tessier method as a routine means to establish solubility profiles for the preliminary evaluation of unknown and reactor derived radionuclide-contaminated materials. The information generated is necessary to permit a better prediction of environmental and human health risk arising from currently 'unknown' radiologically contaminated materials [22]. Implementation of a simple yet robust standardized radionuclide sequential extraction method such as this will further allow meaningful inter- and intra-laboratory comparisons to be conducted [17].

EXPERIMENTAL

Samples and Sample Preparation

Natural uranium dioxide (UO_2) - a milled black powder; thorium dioxide (ThO_2) – a white crystalline milled powder and irradiated UO_2 fuel particulate were collected from the Fuel Development Facility located at the Canadian Nuclear Laboratories (CNL) Chalk River, ON. The irradiated UO_2 fuel particulate was originally collected from a fuel pellet (ID: M73397Z), which was from Pickering Nuclear Generating Station (PNGS), Pickering, ON, and undergoing post-irradiation examination at CNL.   With a reactor residency time of 582 days at 588 kW, the discharge burn up (total energy produced by the nuclear fuel per unit mass) of the irradiated UO_2 fuel was 274 MWd·kg^{-1}U.

The three fuel samples were size fractioned such that each was of a similar size with an average activity median aerodynamic diameter (AMAD) of 2.5 ± 0.5 µm. A Horiba LA-900 laser diffraction analyzer was used to collect particle size distribution (PSD) curves and values for all particulate samples.

Radiochemical Separation Procedure

Although the activity concentration (MBq/g) of both the actinoids (formerly known as actinides) and fission products within the irradiated fuels tested were predicted using CNL fuel code data, confirmatory analyses were conducted following the size-fractioning of the fuel samples. The final activity and isotopic concentrations in the sample were evaluated using a defined radiochemical separation procedure shown by the schematic representation in Figure 18. Following the complete dissolution of three irradiated UO_2 sub-samples, each underwent gamma spectrometric analysis using a coaxial high purity germanium (HPGe) detector with lead shielding (AMETEK/ORTEC). The detection efficiency was calibrated with a multi-gamma source standard and the samples were counted for 4 hours. The irradiated UO_2 fuel samples were then passed through a series of pre-conditioned anion exchange and extraction chromatography columns for the tandem separation of Pu, Am/Cm, U isotopes and ^{90}Sr[23].
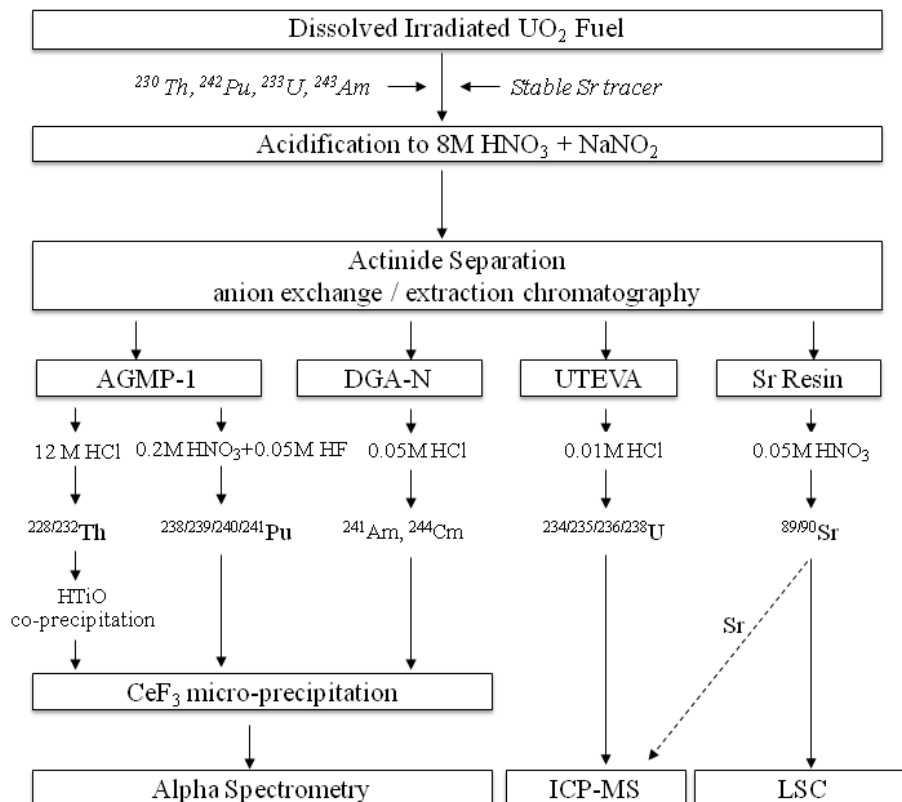
Figure 17 Radiochemical separation procedure for characterization of irradiated UO₂ fuel and for its corresponding solutions from each sequential extraction step. (*thorium isotopes in respect to irradiated fuel, are not included or further discussed in this study.)

Briefly, each sub-sample of irradiated UO_2 fuel suspension obtained was spiked with tracers [243]Am, [233]U, [242]Pu and stable Sr, to enable the evaluation of radiochemical recovery. The samples were dissolved under highly acidic conditions, evaporated to near dryness and re-suspended in 8M HNO_3. Following valency adjustment of the actinoids using $NaNO_2$, the samples were passed through the pre-conditioned anion exchange [AGMP-1M resin (Bio-Rad Laboratories Canada Ltd., Mississauga ON)] and extraction chromatography columns (Eichrom UTEVA, DGA and Sr resins; Eichrom Technologies, Inc., Illinois, USA), for the separation of Pu, Am/Cm, U isotopes and [90]Sr. The columns were rinsed with 8M HNO_3 and split for elution. Per sub-sample, 4 eluate samples (i.e., Pu, U, Am/Cm and Sr) were obtained. The uranium eluate and half of the plutonium eluate underwent ICP-MS analysis of [234, 235, 236, 238]U and [239,240,241]Pu isotopes. All of the americium/curium eluate and the remaining plutonium eluate underwent a CeF_3 micro-precipitation and filtered onto 0.1 µm Resolve™ filters (Eichrom Technologies, Inc.) to prepare thin layer sources for alpha spectrometry. Each sample was counted for 16 h using an Octête Plus® Alpha Spectrometry Workstation (AMETEK/ORTEC Inc., Oakridge, Tennessee, USA). The activity concentrations of [241]Am, [243/244]Cm (the combined activities of both [243]Cm and [244]Cm, as their spectral lines overlap in the alpha spectrum and cannot be separated), [238]Pu and [239/240]Pu (the combined activities of both [239]Pu and [240]Pu, as their spectral lines overlap in the

alpha spectrum) isotopes were reported. For the ^{90}Sr eluate, a fraction was diluted in 0.1M HNO$_3$ and analyzed for stable Sr by ICP-MS. The remainder was mixed with Ultima Gold AB liquid scintillation cocktail for counting on a Hidex 300SL liquid scintillation counter immediately following radiochemical separation.

All measured activities and concentrations were decay-corrected to the sampling date (February 1, 2012) of the irradiated UO$_2$ fuel sample. Since the alpha spectral lines of $^{243/244}$Cm overlap, the two Cm isotopes could not be separately identified by alpha spectrometric analysis. However, it is expected that Cm-244 dominates the combined activity for the two isotopes, as a simulation using high fuel burn-up models predicts that ^{244}Cm would be more than 10 times as abundant as Cm-243 by activity.

Sequential Extraction Method

The sequential extraction method was performed according to Table 5, which provides instructions for each of the five extraction steps. All samples identified were run in triplicate (n=3). With a reagent to sample ratio of 15:1, the selective extraction method used different reagents sequentially applied to obtain the following operationally defined fractions from the materials: exchangeable; acidic or weakly adsorbed; reducible; oxidizable; and residual. This range identifies first those radionuclides that are easily dissolvable and those with subsequently decreased solubility or insolubility under most conditions. Although these five defined steps of the Tessier method were developed to address the speciation and dissolution of complex geological samples (i.e., soils and sediments), they provide a standardised method to compare the solubility, including the biosolubility of other materials. Extraction steps 1to3 of the radionuclide sequential method identifies the percentage fraction of tested materials that are likely to have the highest environmental solubility. Steps 3 and 4 identify fractions that are less soluble and likely to remain associated with the matrix and perhaps remain at the site of environmental deposition. For un-irradiated and irradiated UO$_2$ fuel samples, the dissolved residual fraction was obtained by strong acid digestion using 8M nitric acid (HNO$_3$) with hydrochloric acid (HCl). However, as ThO$_2$ is a "hard-to-dissolve" refractory oxide, 8M HNO$_3$ was used in appropriate combination with a fluorinating agent. As thorium forms a much stronger complex with fluoride ions than with either chloride or bromide ions, ammonium hexafluorosilicate [(NH$_4$)$_2$SiF$_6$] was used to produce thorium in a soluble form (Th^{4+}) prior to analysis.

Table 3 Optimized Sequential Extraction Method

Extraction Step	Reagents*	Temperature (°C)	Concentration (mol/L)	Time (h)
1	$MgCl_2$	25	0.1	1
2	NH_4Ac in 25% (v/v) HAc	50	1.0	2
3	NH_2OH-HCl in 25% (v/v) HAc	70	0.1	6
4	30% (v/v) H_2O_2 in HNO_3 (0.02M)	70	8.8	3
**5	HNO_3 digestion	90	4.0	4

** modifications to ensure all residual particulate is dissolved (i.e. ThO₂ and use of fluorinating agent)

Ac = CH₃COO⁻

The three fuel samples, which were all slightly dampened, were spiked with tracers (fixed masses) to evaluate radiochemical recovery. The tracers ^{233}U and ^{230}Th were added to the unirradiated UO_2 and ThO_2 samples, respectively and ^{243}Am, ^{233}U, ^{242}Pu and stable Sr were added to the irradiated UO_2. All samples were then subjected to the first extraction. The extractions, which are shown in Table 5, commenced with the addition of the first reagent to the sample. The samples were then sealed and placed in a thermostatically controlled shaking water-bath for 1 h at 25°C. Then each sample was centrifuged for 30 minutes at 3000 rpm to collect the aqueous phase for analysis and radiochemical recovery. This process was repeated for the remaining extraction steps, each producing an aqueous phase that could be used to assess radionuclide content. Tracer additions were made at the beginning of each extraction step to monitor radiochemical recovery.

For un-irradiated UO_2 and ThO_2 related aqueous phase solutions produced after each sequential extractions step, ^{238}U and ^{232}Th were separated using a UTEVA (Eichrom Technologies, Inc.) column as indicted in Figure 19 and analyzed using ICP-MS. The aqueous phase obtained from each extraction step from these samples underwent valency adjustment using a 30% H_2O_2 solution. At a flow rate of 1 mL·min^{-1}, the samples were then loaded onto a UTEVA column. Elution of ^{238}U and ^{232}Th was performed using 10 mL of a 0.002 M HCl and 0.03 M HF solution, at a rate of 1 mL·min^{-1} then analyzed for ^{233,238}U and ^{230,232}Th using ICP-MS analysis.
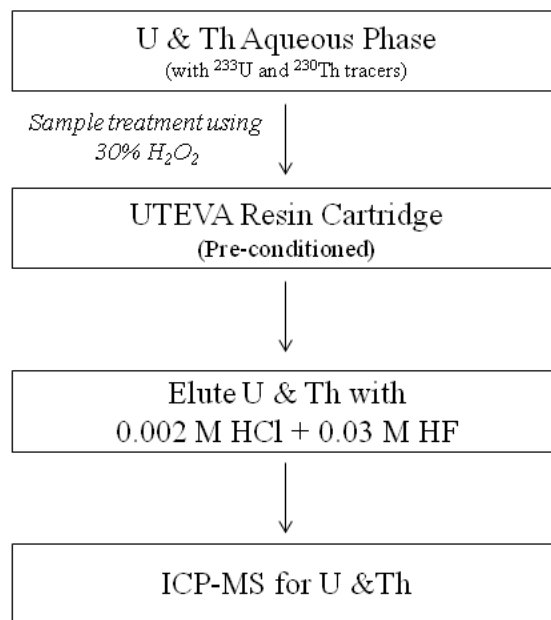
Figure 18 Radiochemical separation procedure for characterization of uranium and thorium isotopes corresponding to un-irradiated UO$_2$ and ThO$_2$ samples.

The aqueous solutions remaining after each sequential extraction step corresponding to irradiated UO$_2$ fuel samples, first underwent gamma spectrometric analysis followed by the radiochemical separation procedure as described in Figure 18.   For each sample, $^{238,239/240,241}$Pu, ^{241}Am, ^{244}Cm, ^{234,235,236,238}U and ^{90}Sr isotopes, along with ^{137}Cs, were measured and elution profiles constructed.

Statistical Analysis

Comparison of either the mass or activity concentrations of the measured radionuclides in each extracted fraction was performed using Student's t-test. This was undertaken to determine if noted differences in the mean values between groups were significant.   The null hypotheses formulated was that there was no difference between means using a 95% confidence interval.

Results and Discussion

Radionuclide characterization before extraction

Before extraction, the average mass of ^{238}U and ^{232}Th in the un-irradiated UO$_2$ and ThO$_2$ samples analysed was 1.04 ± 0.09 mg and 1.01 ± 0.09, respectively.   The activity of each measured radionuclide in the un-extracted, irradiated UO$_2$ samples and their percentage contribution in the total measured activity are given in Table 6.

Table 4 The average radionuclide activity and corresponding percent isotopic contributions in irradiated UO$_2$ fuel samples. [± Standard Error of the Mean (S.E.M]

Isotope	Activity (Bq)	% Activity Contribution
^{234}U	0.21 ± 0.15	<0.01
^{235}U	0.007 ± 0.005	<0.01
^{236}U	0.0127 ± 0.0002	<0.01
^{238}U	0.209 ± 0.187	<0.01
^{241}Am	93.4 ± 12.1	0.3
^{244}Cm	308 ± 24	0.9
^{238}Pu	201 ± 17	0.6
^{239}Pu	77.1 ± 9.5	0.2
^{240}Pu	163.7 ± 27.2	0.5
^{241}Pu	9838 ± 900	28.0
^{90}Sr	7284 ± 250	20.8
^{137}Cs	17127 ± 420	48.8

Radionuclide concentration in the sequentially extracted fractions

Table 7 shows the measured elution profiles for ^{238}U and ^{232}Th resulting from the dissolution of un-irradiated and irradiated UO$_2$ and ThO$_2$ fuel. Figure 20 illustrates the percent cumulative dissolution according to extraction step for each of the fuels. The impact of reactor burn-up (irradiation) on the dissolution of UO$_2$ fuel was evaluated by measuring the amount of ^{238}U in each of the sequentially extracted fractions.

Table 5 Average percent distribution of ^{238}U and ^{232}Th in the fractions obtained by the sequential extraction of un-irradiated UO$_2$, irradiated UO$_2$ and ThO$_2$. [±S.E.M]

Percent Radionuclide Distribution			
Fraction	Un-irradiated UO$_2$ (^{238}U)	Irradiated UO$_2$ (^{238}U)	ThO$_2$ (^{232}Th)
1	1.0 ± 1.0	14 ± 1.0	1.9 ± 0.5
2	10 ± 0.32	2 ± 0.34	0.08 ± 0.01
3	1 ± 0.11	0.5 ± 0.11	0.3 ± 0.02
4	1 ± 0.9	2.5 ± 0.9	0.02 ± 0.001
5	87 ± 2	81 ± 2	97.7 ± 0.4
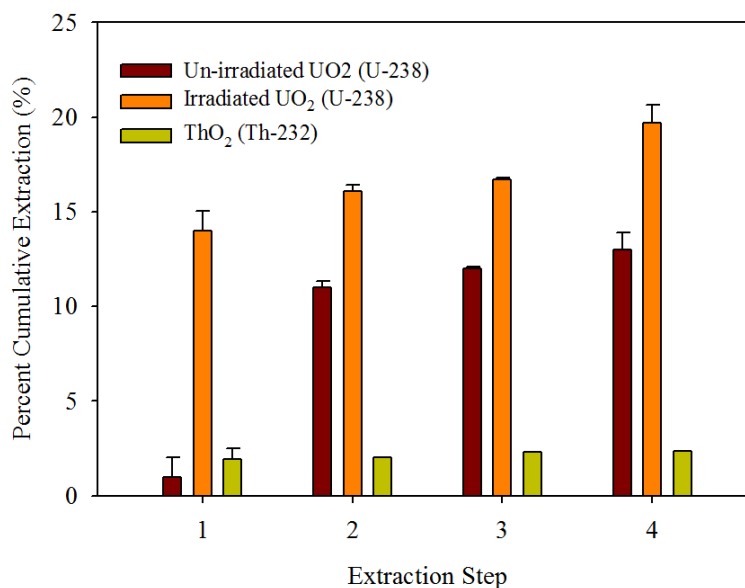
Figure 19 Percent cumulative dissolution according to extraction step for un-irradiated and irradiated UO$_2$ as a measure of U-238 and ThO$_2$ as a measure of Th-232.

Within the collected leachate solutions uranium and thorium most likely exist as the aqueous, divalent uranyl (UO$_2^{2+}$) and tetravalent thorium (Th^{4+}) ions, respectively.   As, the solubility product of uranium species is greater than that of thorium, under similar conditions, it is expected that UO$_2$ will dissolve more readily than ThO$_2$. The first exchangeable extraction fraction was collected using magnesium chloride (MgCl$_2$). This is a neutral salt which is expected to only release weakly bonded metal species associated with the material; these are

easily broken by ion-exchange processes. As shown in Table 3, neither un-irradiated UO_2 nor ThO_2 demonstrated significant solubility in the magnesium chloride solution. Although the amount of ^{232}Th released in the aqueous phase was about an order of magnitude higher than the amount of un-irradiated ^{238}U released this is not thought to be a specific consequence of exposure within the reagent. Instead it is suggested that the greater amount of Th leached was due to the presence of colloidal $ThO_2(aq)$ in the leachate. However, a statistically significant difference was observed between the average percent dissolution of irradiated ^{238}U and un-irradiated ^{238}U in fraction 1: 14 ± 1.0 % and 1.0 ± 1.0 % (*p <0.001*), respectively.

In the aqueous phase of fraction 2, the percent dissolution of un-irradiated ^{238}U was found to be significantly greater than that of irradiated ^{238}U but the cumulative amount extracted remained lower (see Figure 20). No significant amount of ^{232}Th (*p<0.001*) was extracted. In this extraction, ammonium acetate was used to attack those phases considered easily acid-soluble. The pH of this solution was ~5 and was similar to the pH of rain water, which depending on its origin, has a pH range of 5.0-5.6. As the hydrolysis of ThO_2 is thermodynamically unfavourable under most conditions, no significant ^{232}Th dissolution was observed. Along with introducing a mildly acidic pH, UO_2^{+2} is also known to form strong complexes with acetate.   This seemed to have resulted in an increase in the average dissolution of un-irradiated UO_2, with 10 ± 0.32 % of the total ^{238}U being released into the aqueous phase of the fraction. Similar to the percent fraction of irradiated ^{238}U dissolution (14 ± 1.0%) observed in the first fraction, these results suggest that the physical and chemical changes to the fuel following reactor operation (i.e., retention of generated transuranics, production of finely dispersed bubbles within the fuel grains from gaseous fission products and the changes to porosity), affects the fuel solubility behaviour under less aggressive conditions. It appears irradiated UO_2 may be more readily dissolved compared to its un-irradiated form, upon its immediate entry to the environment, releasing ^{238}U from its matrix as a result of natural leaching and dissolution processes. The severity of migration and contamination of surrounding soils, vegetation or ground water however, is influenced by many factors. The mobility of dissolved ^{238}U as uranyl cations can easily be halted by adsorption onto various mineral surfaces or by reduction to its less soluble tetravalent form (U^{+4}) via microbial activity [24].

The mineral phases that will halt dispersal of UO_2^{+2} migration, are similar to those from which UO_2 was originally mined. These include uranyl-oxy-hydrate minerals such as schoepite and studite; or if silica, vanadate or phosphate is present, autonite and carnotite [24].

The percent distribution of dissolved un-irradiated and irradiated ^{238}U and ^{232}Th throughout the remaining fractions as identified in Table 7, were similar for all three fuel samples. No significant differences in percent dissolution in the reaming fractions were observed and the largest percentage present was in the residual 'insoluble' fraction.

Shown in figure 21 are the extraction profiles for the uranium isotopes, ^{234}U, ^{235}U, ^{236}U and ^{238}U from the irradiated U fuel. As expected, all were extracted similarly under the conditions applied, in that the percent dissolution of each uranium isotope was comparable to that of dissolved irradiated ^{238}U throughout all measured fractions with significant dissolution in fraction 1 and the largest percent dissolution identified in the final fraction.
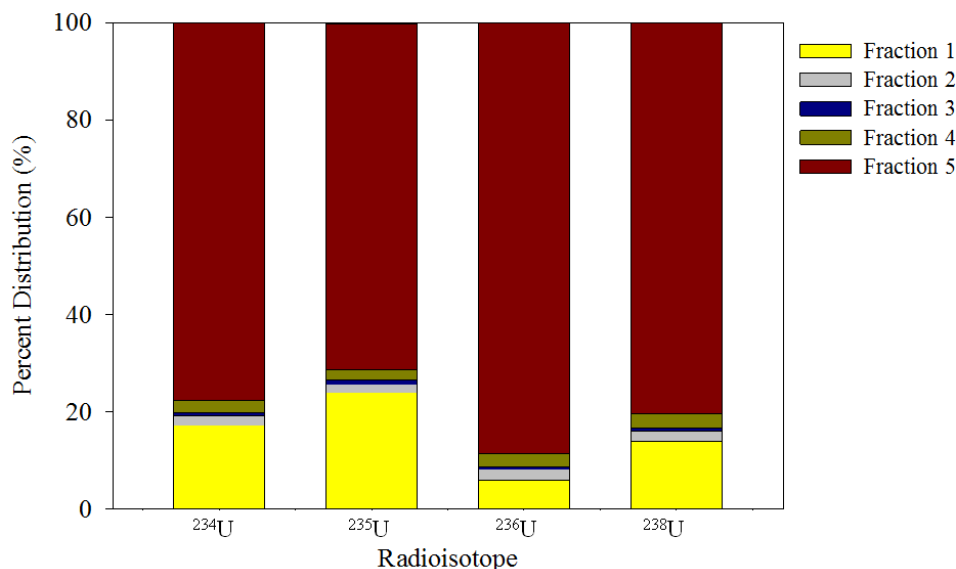
Figure 20 Extraction profiles representing the percent dissolution of uranium isotopes per sequential extraction step from irradiated UO₂ fuel.

The extraction profiles for plutonium isotopes associated with irradiated UO$_2$ fuel are represented in Figure 22. All of the plutonium isotopes were distributed more uniformly between the extracted phases, with a slightly larger percent dissolving in the fourth fraction. With approximately 40% of the total isotopic plutonium concentration likely to be dissolved or leached from irradiated fuel matrix upon accidental release into the environment, evident by the total plutonium in the first three of the five fractions, how these plutonium isotopes behave in the environment will be variable and greatly dependent on local conditions. The mobility of dissolved plutonium will be controlled, by factors such as the type of soil, its composition and physiochemical properties as well as the meteorological conditions. These factors help determine the fraction found to reside in surface soils or those that will migrate deeper being removed by root uptake or other mechanisms.
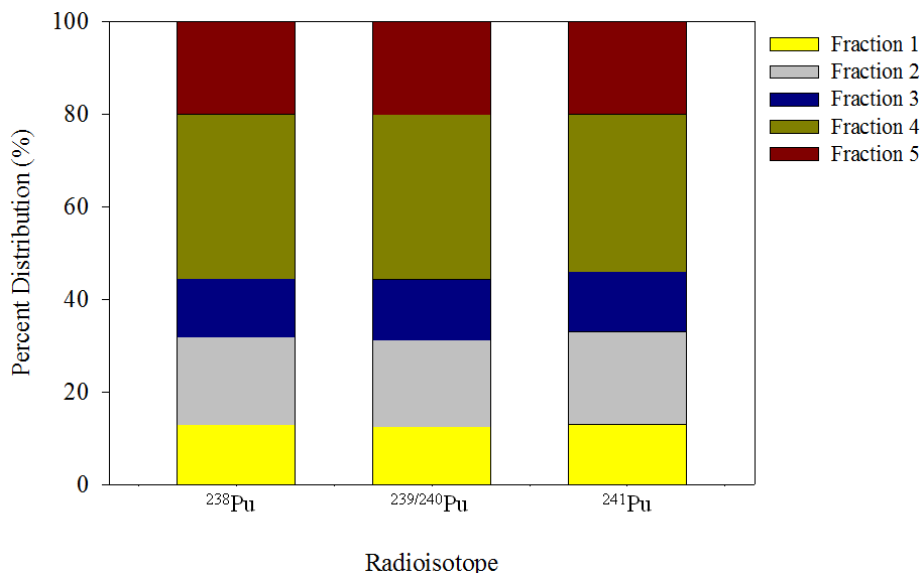
Figure 21 Extraction profiles representing the percent dissolution of plutonium isotopes per sequential extraction step from irradiated UO₂ fuel.

Previous sequential extraction studies performed on contaminated sediment from Sellafield and soil samples surrounding Chernobyl, demonstrate the effect of local conditions on providing different fates for plutonium upon dissolution from the originally-released contamination. The Sellafield sediment, included >40% of the dissolved plutonium in the aqueous phase of fraction 2, which indicates that the majority of the sediment contained plutonium that became bound to carbonate complexes, thus released by slight changes (decrease) of pH. A further 25% of the total plutonium concentration in the sediment was bound to organic material, which was identified by the dissolution of plutonium in fraction 4, whereby when subjected to harsh oxidizing conditions using H_2O_2, plutonium was released. However, the soil sample characterized from Chernobyl, indicated that the largest percent fraction of plutonium present was associated with organics (~75%) [2]. The difference between these two types of contaminated samples in terms of further environmental risk assessment or long term predictions of radionuclide mobility and bioavailability is that the Sellafield sediment contains a fraction of plutonium with a higher level of exchangeability, where slight changes to soil acidity permits the contamination to migrate.

The extraction profiles for the remaining radioisotopes, ^{241}Am, ^{244}Cm, ^{90}Sr and ^{137}Cs, measured in respect to irradiated UO₂ fuel, , are shown in Figure 23, and indicate that the largest percent dissolution for each isotope appeared in the aqueous phase of fraction 4, at 62±4%, 59±2%, 75±4% and 65±2%, respectively. However, significant dissolution was also observed in fractions 1-3 for ^{241}Am, ^{244}Cm, ^{90}Sr and ^{137}Cs, providing a sum of 32.5%, 35%, 21% and 30.5%, respectively. This corresponds to the percentages most likely to be most easily dissolved from the irradiated fuel, when deposited into the environment. Although further experimental efforts will aid in defining how these dissolved fractions behave in local facility environments, the results permit for some estimates to be made. It is known, that cesium for example, which has

no biological role, enters biological systems with ease. It is also known that adsorption plays a detrimental role in the mobility of ^{137}Cs when released into soil. Clay minerals, specifically, illites and vermiculites, have strong affinities for cesium [25,26]. Although some soils adsorb cesium quite efficiently (possibly irreversibly) in some environmental systems, ^{137}Cs continues to remain bio-available years after contamination, therefore continually being environmentally and biologically available.   Therefore, soils that perhaps do not contain enough clay minerals to immobilize ^{137}Cs will permit its further migration and bioavailability. It has also been reported, that despite the weak, non-specific interaction between soil organic matter and cesium, the organics will decrease the affinity of cesium to clay minerals and therefore, reduce their ability to immobilize cesium; thus, providing ^{137}Cs available for soil biota or plant uptake over a long period of time.
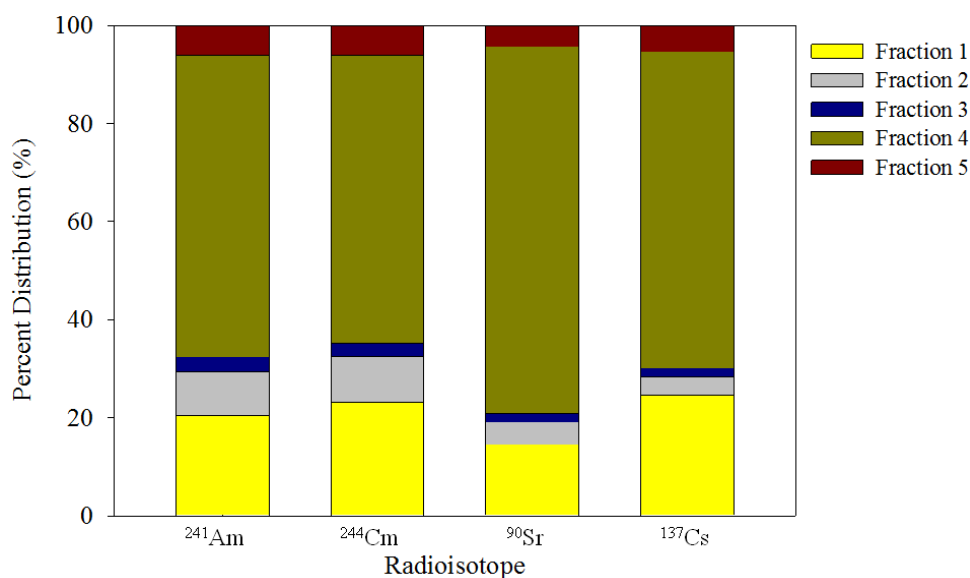
Figure 22 Extraction profiles representing the percent ^{241}Am, ^{244}Cm, ^{90}Sr and ^{137}Cs dissolution per sequential extraction step from irradiated UO$_2$ fuel.

Although a similar and fairly uniform distribution of ^{241}Am, ^{244}Cm, ^{90}Sr and ^{137}Cs among extraction phases was seen, the differences observed between these and the plutonium isotope extraction profiles in Figure4, were found to be significant. The dissolution of ^{241}Am, ^{244}Cm and ^{137}Cs in fraction 1 was significantly greater than that of all Pu isotopes ($p<0.001$). However, the dissolution of ^{238}Pu, $^{239/240}$Pu and ^{241}Pu in fraction 2 at 19±3%, 18.5±2% and 20±3%, respectively, was significantly greater than that of the other radioisotopes dissolved in that fraction ($p<0.001$). The plutonium dissolution in fraction 3 was also found to be significantly greater ($p<0.001$). During the reactor irradiation process, the steep thermal gradient present in a single fuel pellet, from hundreds of degrees Celsius at the rim to nearly 1800ºC in the center, causes grain coarsening and micro-fracturing. This further causes the radionuclide distribution to be quite heterogeneous.   Fission products such as volatile ^{137}Cs and ^{90}Sr are known to migrate and concentrate at the grain boundaries and fractures within the fuel, while actinides will tend to

become incorporated into the UO_2 fuel structure [27,6]. The results shown here, suggest that the increased percent of the total dissolved Am, Cm, Sr and Cs in fraction 1, is likely a result of these radionuclides being present in higher concentration at or near the grain boundary locations where there is also an increase in fuel porosity. As the percent dissolution values for each of the specified radionuclides were similar, the average activity losses (dissolution) described above suggest that these radionuclides (^{241}Am, ^{244}Cm, ^{90}Sr and ^{137}Cs), unlike plutonium, were released by the bulk dissolution of the fuel matrix rather than by selective leaching. This conclusion was confirmed for the individual radionuclides by plotting percent dissolution of one radionuclide against the other. The results are presented in Figure 24.
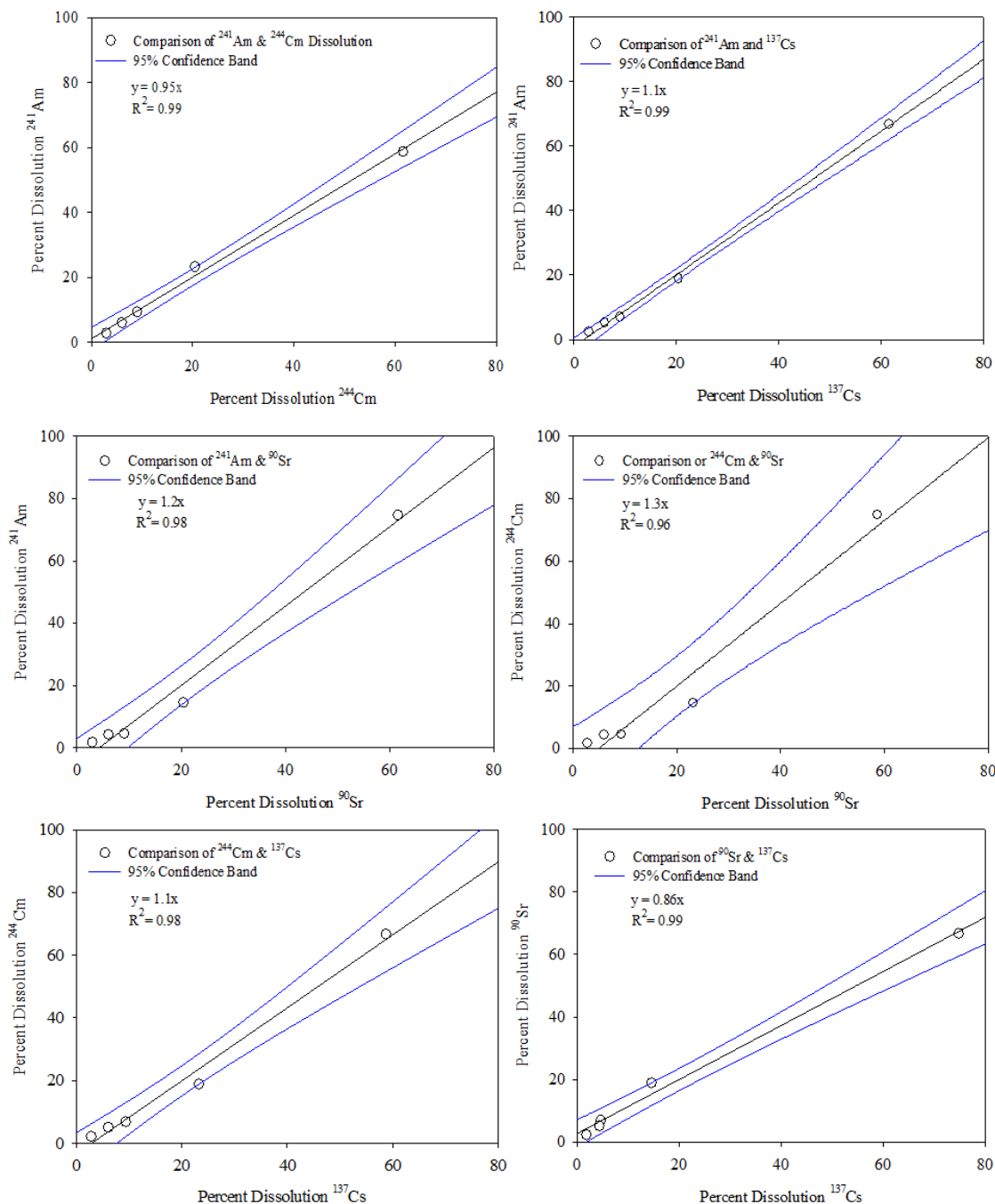
Figure 23   Comparison of radionuclide dissolution, demonstrating the radionuclides were released by the bulk dissolution of the fuel matrix.

The slope of the regression lines shown, are considered fully consistent with the suggestion that these radionuclides were lost at the same rate.

Conclusions

Demonstrated in this study, was the effect of reactor burn-up on the dissolution of UO_2 fuel, in that it provides a more 'soluble fraction' of uranium due to the structural and chemical changes exhibited during reactor operation. The percent fractions of the associated actinides and activation/fission products, likely to dissolve from the irradiated fuel matrix upon its accidental release into the environment, were predicted. It is also suggested that the dissolution results reported for ^{241}Am, ^{244}Cm, ^{90}Sr and ^{137}Cs, was a result of the dissolution of the bulk irradiated UO_2 fuel structure. This is based on the similarities of percent radionuclide fractions measured and the regression analyses that were performed. Plutonium however, exhibited a solubility profile that was found to be significantly different than all of the other radionuclides measured. This result was consistent with other laboratory experimental and bioassay measurements which showed that plutonium has a different dissolution behavior than these specific radionuclides, in a simulated lung environment.

Although solubility, particle size, kinetics, the nature of the geochemical environment and meteorological conditions will affect the availability of these radionuclides in soil, water and for plant or animal uptake, using a sequential extraction method such as the one described, provides itself as a useful screening tool in the nuclear industry. It provides a standardized means of obtaining material specific information that is necessary to allow for an improved assessment of environmental and human health risk from released radiological hazards. As the best predictor of environmental and human health risk from such materials is currently by the direct measurement of solubility in specific locally defined environments (local soils, groundwater, and lung-serums), efforts are being made to obtain such valuable information.

References

1. Smodis B, Strok M, Cerne M (2014) Radioecology around a closed uranium mine. Journal of Radioanalytical and Nuclear Chemistry 299 (1):765-771. doi:10.1007/s10967-013-2697-2

2. Komosa A (2002) Study on geochemical association of plutonium in soil using sequential extraction procedure. Journal of Radioanalytical and Nuclear Chemistry 252 (1):121-128. doi:10.1023/a:1015252207934

3. Pulford ID, Allan RL, Cook GT, MacKenzie AB (1998) Geochemical associations of Sellafield-derived radionuclides in saltmarsh deposits of the Solway Firth. Environ Geochem Health 20 (2):95-101. doi:10.1023/a:1006597809373

4. Štrok M, Smodiš B (2013) Partitioning of natural radionuclides in sediments around a former uranium mine and mill. Journal of Radioanalytical and Nuclear Chemistry 297 (2):201-207. doi:10.1007/s10967-012-2364-z

5. Hedin A (1997) Spent nuclear fuel how dangerous is it: a report from the project "description of risk". Svensk kärnbränslehantering AB/Swedish Nuclear Fuel and Waste Management. Available via http://worldcat.org. http://books.google.com/books?id=RQ5SAAAAMAAJ.

6. Lewis BJ, Hunt CEL, Iglesias FC (1990) Source term of iodine and noble gas fission products in the fuel-to-sheath gap of intact operating nuclear fuel elements. J Nucl Mater 172 (2):197-205. doi:http://dx.doi.org/10.1016/0022-3115(90)90438-S

7. Burns PC, Ewing RC, Navrotsky A (2012) Nuclear Fuel in a Reactor Accident. Science 335 (6073):1184-1188. doi:10.1126/science.1211285

8. Popplewell DS (1995) Biokinetics and Absorption of Actinides in Human Volunteers: A review. National Radiological Protection Board 46 (5):279-286

9. Menetrier F, Taylor DM, Comte A (2008) The biokinetics and radiotoxicology of curium: a comparison with americium. Appl Radiat Isot 66 (5):632-647

10. Salbu B (2009) Fractionation of radionuclide species in the environment. Journal of Environmental Radioactivity 100 (4):283-289. doi:10.1016/j.jenvrad.2008.12.013

11. Salbu B, Krekling T, Oughton DH (1998) Characterisation of radioactive particles in the environment. Analyst 123 (5):843-849. doi:10.1039/a800314i

12. Skipperud L, Salbu B (2015) Sequential extraction as a tool for mobility studies of radionuclides and metals in soils and sediments. Radiochim Acta 103 (3):187-197. doi:10.1515/ract-2014-2342

13. Bertelli L, Puerta A, Wrenn ME, Lipsztein JL (1997) Specific absorption parameters for uranium octoxide and dioxide applicable to the ICRP Publication 66 respiratory tract model. Journal of Radioanalytical and Nuclear Chemistry 226 (1-2):233-239. doi:10.1007/bf02063654

14. Tessier A., Campbell P. G. C., Bisson M. (1979) Sequential extraction procedure for the speciation of particulate trace metals. Analytical Chemistry, vol 51.

15. Outola I, Inn K, Ford R, Markham S, Outola P (2009) Optimizing standard sequential extraction protocol with lake and ocean sediments. Journal of Radioanalytical and Nuclear Chemistry 282 (2):321-327. doi:10.1007/s10967-009-0183-7

16. Schultz M., Inn KGW, Lin ZC, Burnett WC, Smith G, Biegalski SR, Filliben J (1998) Identification of radionuclide partitioning in soils and sediments: Determination of optimum conditions for the exchangeable fraction of the NIST standard sequential extraction protocol. Applied Radiation and Isotopes 49 (9-11):1289-1293. doi:10.1016/S0969-8043(97)10062-8

17. Schultz MK, Burnett WC, Inn KG, Thomas JW, Lin ZC (1996) New Directions for Natural-Matrix Standards - the NIST Speciation Workshop. Radioactivity and Radiochemistry 7 (1):9-12. doi:10.1016/S0969-8043(97)10062-8

18. Demkowicz PA, Jerden JL, Cunnane JC, Shibuya N, Baney R, Tulenko J (2004) Aqueous dissolution of urania-thoria nuclear fuel. Nucl Technol 147 (1):157-170

19. Schultz MK, Burnett WC, Inn KGW (1998) Evaluation of a sequential extraction method for determining actinide fractionation in soils and sediments. Journal of Environmental Radioactivity 40 (2):155-174. doi:10.1016/s0265-931x(97)00075-1

20. Health effects of occupational exposure to uranium: do physicochemical properties matter? (2014). Int J Radiat Biol 90 (11):1104-1113. doi: 1110.3109/09553002.09552014.09943849.

21. Blanco P, Vera Tomé F, Lozano JC (2004) Sequential extraction for radionuclide fractionation in soil samples: A comparative study. Applied Radiation and Isotopes 61 (2-3):345-350. doi:10.1016/j.apradiso.2004.03.006

22. Elless MP, Armstrong AQ, Lee SY (1997) Characterization and solubility measurements of uranium-contaminated soils to support risk assessment. Journal Name: Health Physics; Journal Volume: 72; Journal Issue: 5; Other Information: PBD: May 1997:Medium: X; Size: pp. 716-726

23. Dai X, Kramer-Tremblay S (2011) Sequential determination of actinide isotopes and radiostrontium in swipe samples. Journal of Radioanalytical and Nuclear Chemistry 289 (2):461-466. doi:10.1007/s10967-011-1096-9

24. Suzuki Y, Kelly SD, Kemner KA, Banfield JF (2003) Microbial populations stimulated for hexavalent uranium reduction in uranium mine sediment. Appl Environ Microbiol 69 (3):1337-1346. doi:10.1128/aem.69.3.1337-1346.2003

25. Cipakova A (2005) Migration of Radiocaesium in individiual parts of the environment. Nukleonika 50:19-23

26. Stautnton S, Dumat C, Zsolnay A (2002) Possible role of organic matter in radiocaesium adsorption in soils. Journal of Environmental Radioactivity 58 (2-3):163-173. doi:10.1016/s0265-931x(01)00064-9

27. Kleykamp H (1985) The chemical state of the fission products in oxide fuels. J Nucl Mater 131 (2):221-246. doi:http://dx.doi.org/10.1016/0022-3115(85)90460-X

6.2   Static Solubility Test

Inhaled exogenous particulate will enter the respiratory tract and leave the lung by either mechanical clearance or by partially dissolving in the fluid lining of the lungs. This is followed by a combination of events such as retention, re-distribution and excretion in the rest of the body. The rate at which dissolution of the inhaled particulate occurs will directly affect the retention time in the lung and where the radionuclide is deposited in the rest of the body, and hence the fraction available for re-distribution to target tissues and organs. The consequential radiation dose is dependent on these events and the tissue exposure time. When evaluating dose to an individual and for dose modelling, the ICRP recommends the use of experimentally determined solubility coefficients [2, 21]. The static method is one of the most widely used methods designed to obtain such information by testing the *in vitro* biological solubility of a material. The method uses simulated lung fluid (SLF) as the solvent/media to investigate the lung solubility as a result of an inhalation exposure. The SLF mimics the chemical composition of the fluid lining of the human lungs by including significant concentrations of complexing anions, carbonates, sulphate and phosphates, and also has a neutral physiological pH (fluid lining of the lung: 7.2–7.4). The SLF composition selected for the study in Table 8 is the most commonly used composition found in the literature [4, 22].

Table 6 Serum Ultra-filtrate (SUF) recipe for simulated lung fluid

Chemicals	Concentration (Mol·L^{-1})	Mass (g)
NaCl	0.116	6.7790
NH$_4$Cl	0.010	0.5349
NaHCO$_3$ (designated as "bicarbonate" or HCO$_3^-$)	0.027	2.2683
Glycine	0.005	0.3754
L-Cysteine	0.001	0.1212
NaC$_6$H$_5$O$_7$ (designated as citrate)	0.0002	0.0428
CaCl$_2$	0.0002	0.0222
H$_2$SO$_4$	0.0005	0.0491
NaH$_2$PO$_4$ (designated as "phosphate" or PO$_4$)	0.0012	0.1439
DTPA (diethylenetriaminepentaacetic acid) *chelating agent not present in serum, but added to decrease the amount of dissolved actinide ions 'sticking' to the walls of the container*	0.0002	0.0787
Alkylbenzyldimethyl ammonium chloride: this is an antibacterial agent not present in serum but added for longer duration studies	*50 ppm*	*0.05*

In the basic design of the static test system, the material is confined between two membrane filters of a specific pore size. Figure 25 illustrates the concept of the static system, where the filters are visibly secured between two tight-fitting polypropylene rings while the top and bottom surfaces of the filter remain exposed to the biological fluid. The holder containing the membrane-particle assembly is then placed into a vessel containing a known volume of fluid. At specific times, the assembly is removed using a retrieval instrument, and the solvent is collected and analyzed for the dissolved radionuclides.
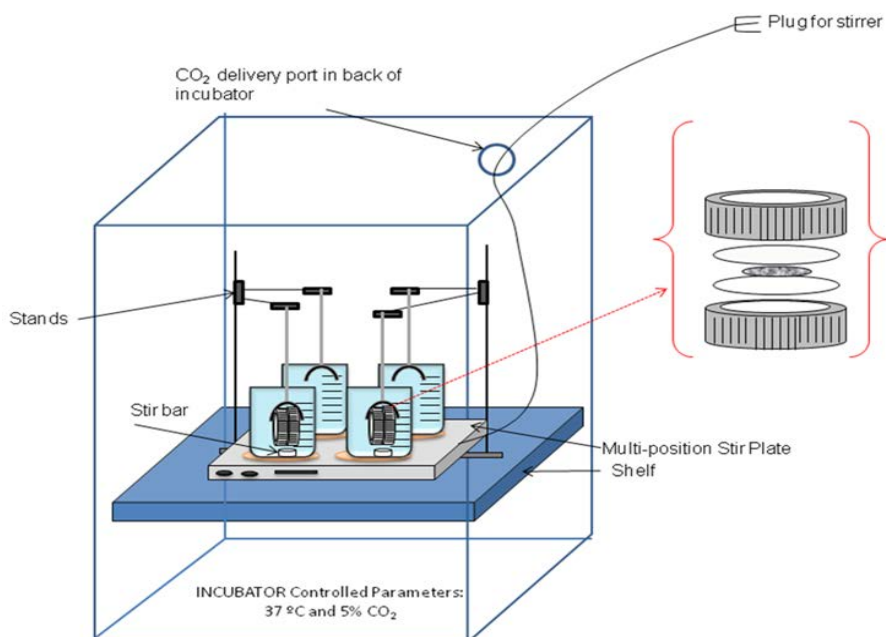
Figure 24 Illustration of a static dissolution cell concept.

The actual set up for the static system used in this study was designed and constructed as shown in Figure 26. The apparatus included an incubator to maintain a controlled temperature of 37°C and a controlled neutral pH by the delivery of 5 % CO_2 in air. Inside the incubator is a multi-position stir plate on which beakers containing the serum ultra-filtrate (SUF) solution and a magnetic stir bar are placed at each of the 4 stir-positions. Located next to the stir plate are retort stands from which the sample holders containing the test material are suspended.

Figure 25 Static test set-up within an incubator for a controlled environment.

Both un-irradiated UO_2 and ThO_2 fuel solubility was measured using this set up. For these tests, a starting mass of 0.52 mg of un-irradiated UO_2 and 1.01 mg of ThO_2 sized particulates in water were strategically vacuum-filtered onto 47 mm diameter filters (pore size 0.1 μm) as shown in Figure 27. This ensured the sample would be deposited in the center of the filter, allowing for easy assembly of the holder with no cross-contamination and importantly eliminating the particles ≤ 0.1 μm that would easily be released through the pores once submerged in the SLF.

Vacuum filtered UO_2

Sample chamber with UO_2 tightly confined between 2 filters
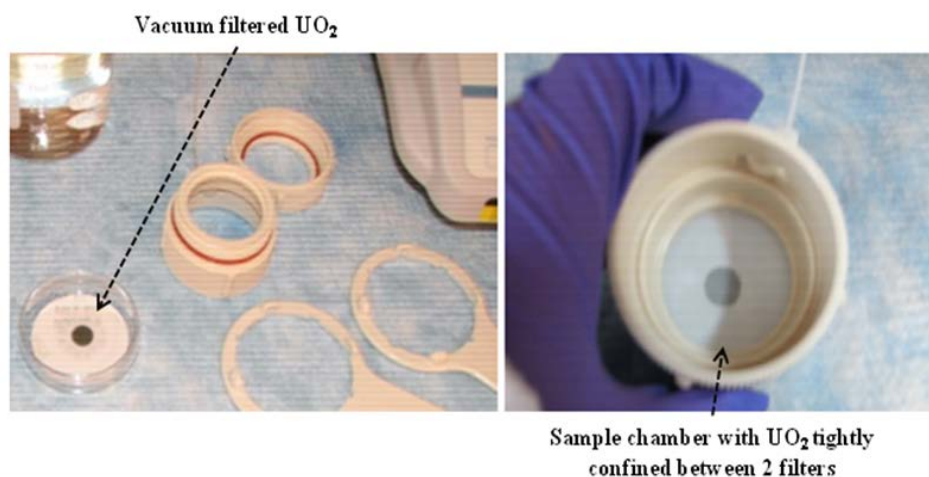
Figure 26 Static Test sample holder. Samples are confined between two filters (pore size <0.1 μm). (Un-irradiated UO_2 is shown in these images)

For each test, 300 mL of the SUF solution was placed into the beakers, along with a stir bar for mild agitation and brought to 37°C inside the incubator. The pH was monitored to ensure that a physiological pH was maintained. The sample, confined in the holder, was then submerged and secured to the retort stand using a polypropylene attachment as previously shown. The times for sample collection are listed in Table 9. At each time point, the total volume of the SUF solution and dissolved radionuclide was collected, and the sample holder was re-submerged into a new beaker containing another fresh volume (300 mL) of SUF solution, already at a temperature of 37°C.

Table 7 Sample collection times for Static Test.

Experimental Time Points	(hours)
0 – controls	48
1	72
2	168
3	336
7	504
24	672

Three replicate (n=3) tests were completed for un-irradiated UO_2 and for ThO_2. For all samples at each time-point, the dissolved uranium and thorium were separated from the high salt matrix of the SLF by using anion exchange resins as shown in Figure 28. A rapid uranium analysis procedure and rapid thorium analysis procedure, as established by X. Dai et al. at CNL, were used for this purpose [23, 24].
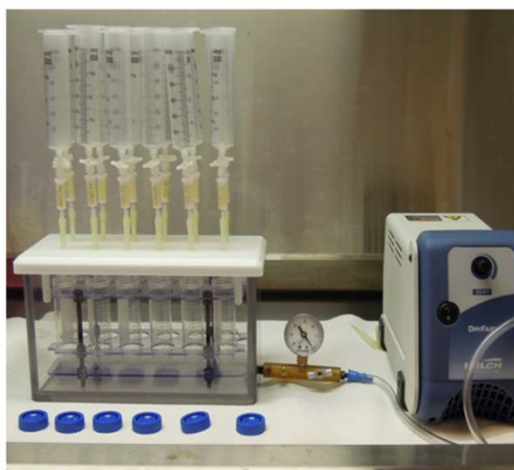
Figure 27 Column separation using anion-exchange resins for uranium and thorium extraction prior to analysis.

Chemical recovery was monitored by using uranium-233 and thorium-230 tracers (by mass) for the UO_2 and ThO_2 samples, respectively. The filters were ashed, and the residual UO_2 and ThO_2 digested and analyzed for mass balance/sample recovery. Specifically, for each un-irradiated UO_2 sample collected at the assigned times, 20 mL sub-fractions were collected. The chemical recovery was monitored by using a U-233 reference standard (*233-U-12-0-RS-1*), which contained an activity concentration of 0.9283 Bq·g^{-1} (2.604 ng·g^{-1}). For each of the three replicate experiments and prior to U-233 tracer addition (by mass), the pipette was calibrated such that the mass added was precise and consistent between all sub-fractions (0.002 σ; U-233).

Each sample underwent radiochemical separations for uranium-238 using a Dowex 1X8 anion resin (Cl- form, 200-400 mesh, Eichrom Technologies). All samples were analyzed by ICP-MS (Analytical Chemistry Branch, CNL). For each ThO_2 sample collected at the assigned times, chemical recovery was monitored by using a Th-230 reference standard (*230-Th-09-0-RS-1-SS-3*), which contained an activity concentration of 8.103 $Bq \cdot g^{-1}$ (1.0366 $ng \cdot g^{-1}$). Again, the pipette was calibrated such that the mass added was precise and consistent between all sub-fractions (0.0002 σ; Th-230). Each sample underwent radiochemical separations using TRU resin 2 mL cartridges (Eichrom Technologies). All separated samples were analyzed by ICP-MS (Analytical Chemistry Branch, CNL).

6.2.1   Results & Discussion

In Figure 29, the data is represented as the percent retained fraction versus elapsed time in hours. The data were fit with single or double exponential equations to evaluate the dissolution coefficients. Table 6 further indicates the percent retention of un-irradiated UO_2 and ThO_2, and corresponding half times and dissolution rates. [Note: for uranium, the blank contains <0.1% U of the lowest recorded value]. Uranium dissolution showed both a fast and slow component, and Th, a single slow component.
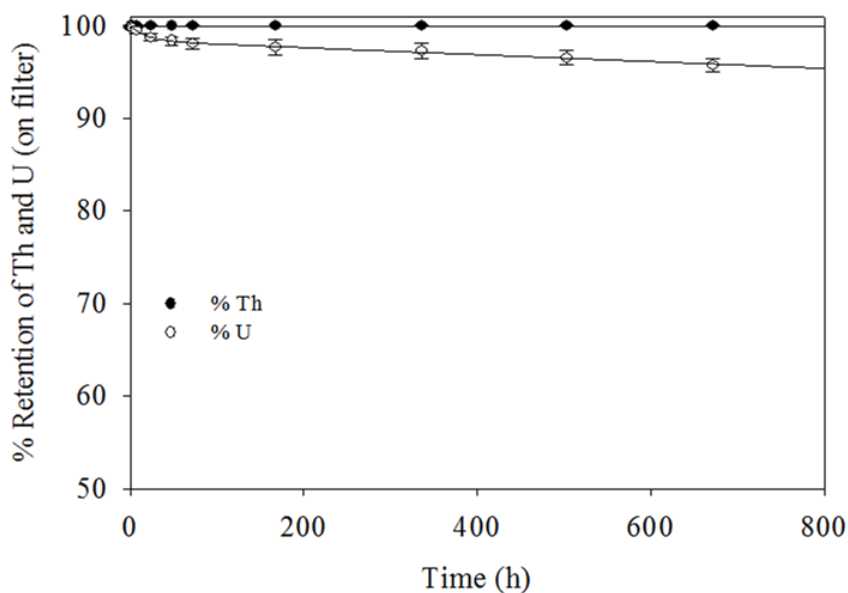
Figure 28 Percent retention of un-irradiated UO₂ and of ThO₂.

For un-irradiated UO_2, approximately 1.6% of the total uranium was found to dissolve with a T½ of 13 d or dissolution rate of approximately 0.052 d^{-1}, with the remaining 98.4% dissolving with a longer T½ of 17,865 d. For ThO_2, all material was evaluated to be retained for an extended period of time with a T½ of 5.5×10^5 d.

Table 8 Summary of the results obtained from the in vitro static test for respirable sized un-irradiated UO₂ and ThO₂.

Radionuclide	Clearance Component	*In Vitro* Static Test		
		Percent (%) Clearance	half life $T_{1/2}$ (d)	Rate (d^{-1})
U	Fast	1.6	13	5.2×10^{-2}
	Slow	98.4	1.8×10^4	3.9×10^{-5}
Th	Slow	>99.9	5.5×10^5	1.3×10^{-6}

It is recommended that material-specific rates of absorption should be used for compounds for which reliable experimental data exist. For other compounds, default values of parameters are recommended. The default ICRP Publication 66 parameters for solubility classification are identified in Table 11.

Table 9 Default ICRP Publication 66 parameters for the solubility model[2].

ICRP Publication 66 Absorption Type	F (*fast*)	M (*moderate*)	S (*slow*)
MODEL PARAMETERS: **Fraction dissolved rapidly,** f_r	1	0.1	0.001
DISSOLUTION RATE: **Rapid,** S_r **(d⁻¹)**	100	100	100
Slow, S_s **(d⁻¹)**	-	0.005	0.0001

Given the dominance of the slow dissolving fraction, it is reasonable to assign S as the Solubility Class for uranium oxide. This is clearly shown in Figure 30 by the proximity of the fitted uranium data to the solubility plot for Type S material; the plot for Type M material is also shown for reference. Similar to uranium dioxide, the k_s value of 1.3×10^{-6} d⁻¹ for thorium oxide is also consistent with an ICRP Solubility Class of S.
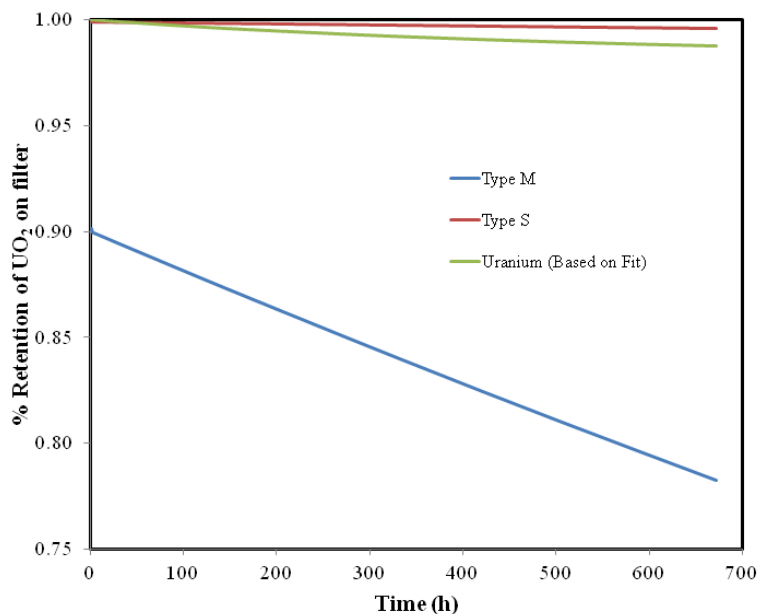
Figure 29 Percent retention of Un-irradiated UO$_2$ on filter.

The static test design is known to have its flaws. The equilibrium between solid and dissolved states in this test set up is one issue that would directly affect the dissolution of the material. This is problematic when trying to calculate the true dissolution rate of a material. The test set up also lacks the feature of fluid mobility, interacting with the particles in a manner that would occur *in vivo* (i.e., mucus flow throughout the trachea-bronchial tree of the lungs). The absence of fluid mobility is expected to further contribute to a decrease in dissolution. The design of the set up also guarantees that a significant fraction of the dissolved sample (i.e., U and Th) will become adsorbed onto the surfaces of the apparatus being used. To remedy these issues, a dynamic system (flow test) was constructed at CNL. The conceptual design of the system is shown in Figure 31.

1. 60 ML DISPOSABLE SYRINGE

2. LUER LOCK ADAPTER

3. 1/16' INTERIOR DIAMETER PVC TUBING

4. INCUBATOR

5. SWINNEX FILTER HOLDERS WITH 25MM 0.1 µM MILLIPORE FILTER

6. DISPOSABLE PIPETTE TIP

7. 50 ML CENTRIFUGE TUBE
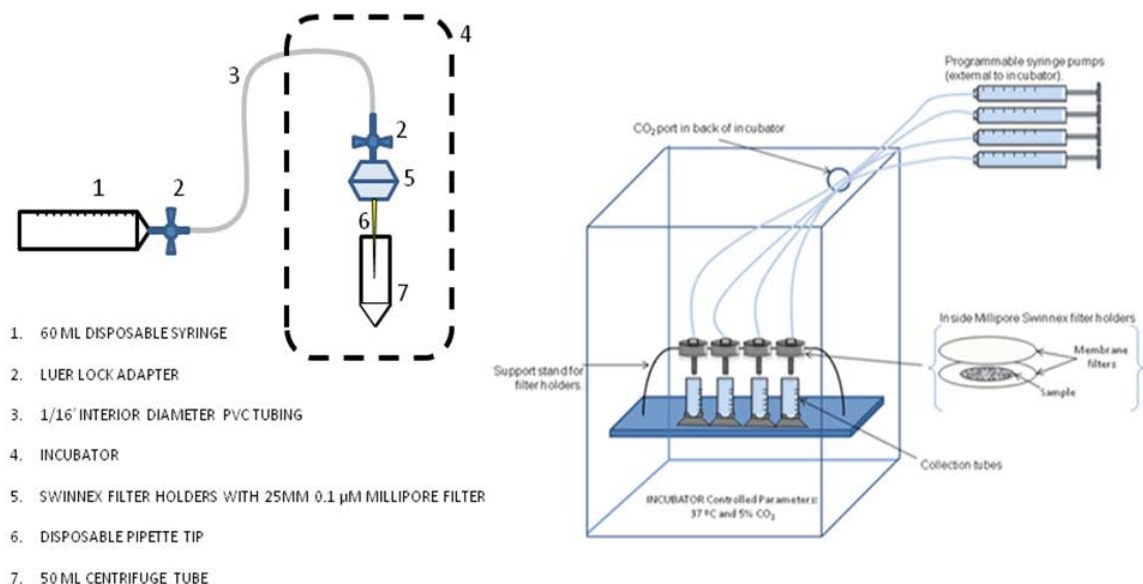
Figure 30 Concept and design for the flow test.

6.3   Flow test

The flow test is an enclosed system which moves simulated lung fluid at a rate comparable to the fluid lining of the lungs, interacting with the material enclosed in a chamber. The design eliminates the equilibrium concern between solid and dissolved states and sample loss due to significant adsorption to the equipment used in the static test. This system was designed to best simulate the conditions of the human lung environment and will provide improved solubility data.

Figure 32 represents the experimental flow test set up with four samples: two un-irradiated UO_2 sub samples and two irradiated UO_2 fuel ID M73397Z. For this test, each sample was placed within the flow chambers, confined between two membrane filters. At a flow rate of 0.46µL/min pre-set on the programmable syringe pump, a temperature of 37 ± 0.5 ^{0}C and pH of 7.4 ± 0.2, simulated lung fluid was passed through the flow chambers to permit interaction with the samples with dissolved fractions collected in a centrifuge tube. At each time point (24, 48, 72, 168, 336, 504 and 720 h), the dissolved fractions were collected. Gamma spectrometric analysis was carried out on each fraction. The detection efficiency was calibrated with a multi-gamma source standard and the samples were counted for 4 hours.

Each fraction collected and measured by gamma spectrometry was then diluted to 20 mL using 8M HNO_3, ready for a 4 column radiochemical separation as previously discussed.

Figure 31 Experimental set up for the flow test. Flow rate: 0.46 µL/min; Temperature: 37 ± 0.5 ^{0}C; pH: 7.4 ± 0.2; Time points 24, 48, 72, 168, 336, 504 and 720 h.

6.3.1   Results & Discussion

Figure 33 demonstrates the percent bulk dissolution of irradiated and un-irradiated UO_2 fuel as a measure of dissolved U-238 at various time points extending over 1 month. As listed in Table 12, 5% of the un-irradiated UO_2 dissolved with a $T_{1/2}$ of 267 d, while the largest fraction of 95% dissolved over a much longer period of time with a $T_{1/2}$ of 1.0×10^5 d. For irradiated UO_2, 12% dissolution of the material exhibited a $T_{1/2}$ of 72 d, with 88% at 3.8×10^4 d.
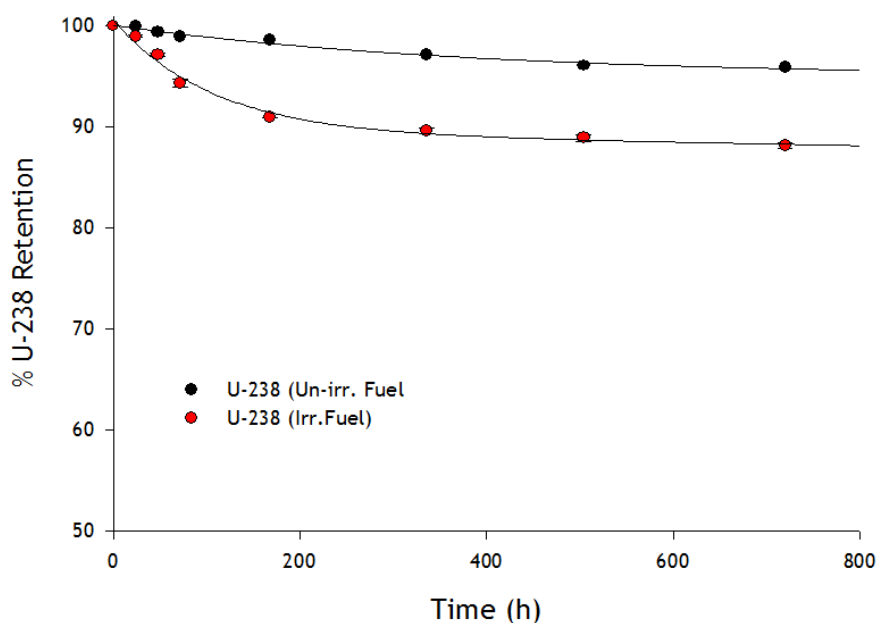
Figure 32 Bulk un-irradiated and irradiated UO$_2$ dissolution as a measure of dissolved U-238 in simulated lung fluid.

Table 10 Radionuclide Dissolution

	Slow Dissolution Component			Fast Dissolution Component		
Radionuclide	f_s	k_s (d^{-1})	$t_{1/2}$ (d)	f_r	k_r (d^{-1})	$t_{1/2}$ (d)
U-238 (un-irradiated)	0.95	6.9E-06	1.0E+05	0.05	2.6E-03	267
U-238 (irradiated)	0.88	1.8E-05	3.8E+04	0.12	9.6E-03	72

With respect to the dissolution/solubility behaviour of a material, the ICRP provides that for a solubility Type S material, one is to assume that the majority of the inhaled material has a dissolution rate of 0.0001 d^{-1} or 7000 d. For a Type M intermediate material, it is assumed that ≥10% has a dissolution rate of approximately 0.005 d^{-1} or 140 d, and for a Type F material, it is considered readily soluble (T ½ 10 minutes).

According to Figure 33, with 95% of the bulk un-irradiated UO$_2$ fuel having a T$_{1/2}$ >7000 d, a Type S material classification is to be assigned. This agrees with the literature on UO$_2$ solubility, as it is well documented, and it is also in accordance to ICRP recommendations for this material. However, with >10% of bulk irradiated UO$_2$ having a T$_{1/2}$ <140 d, a Type M material

classification would be assigned, indicating that this material would have intermediate solubility upon deposition in the lung.

Currently, due to the lack of data surrounding the biological solubility of irradiated UO_2 fuel following an intake, the assumed solubility classification and parameters for dosimetric assessments are applied for un-irradiated and irradiated UO_2 fuel particulates. Although we have expected this to be inappropriate both based on the changes in chemistry and physical structure of the fuel after irradiation, the results shown here demonstrate a biological dissolution that is significantly different for UO_2 fuel following burn up. The results demonstrate the benefit of this work for improving bioassay monitoring and assigned dosimetry to an individual, as it can be used to further predict the retention and excretion following an intake. Furthermore, custom *in vitro* simulated lung dissolution studies are an easy and cost effective way to obtain this material specific information.

Figure 34 provides the individual dissolution curves for Pu-238, 239/240 and 241, Am-241, Cm-244, and Sr-90 and Cs-137 from the irradiated UO_2 fuel ID M73397Z sample matrix. Table 13 lists the percent dissolution values and corresponding half-lives ($T_{1/2}$) in days for each. The results demonstrated that all isotopes of Pu, except Pu-241, displayed two component dissolution, with 1% dissolution over 100 d and 110 d and 99% with a $T_{1/2}$ of 7.6×10^4 d and 1.4×10^4 d, for Pu-238 and Pu-239/240, respectively. As for Pu-241, >99% dissolution was observed with a $T_{1/2}$ of 7.0×10^3 d.   Similarly, Cs-137 observed a >99% dissolution with a $T_{1/2}$ of 1.8×10^4 d. Although both Am-241 and Sr-90 exhibited two-component dissolution, larger fractions of approximately 10% were observed to dissolve at a rate of 0.0084 d^{-1} and 0.0074 d^{-1}, respectively. Curium-244 also exhibited a faster component, where 12% dissolution was observed at a rate of 0.027 d^{-1}.
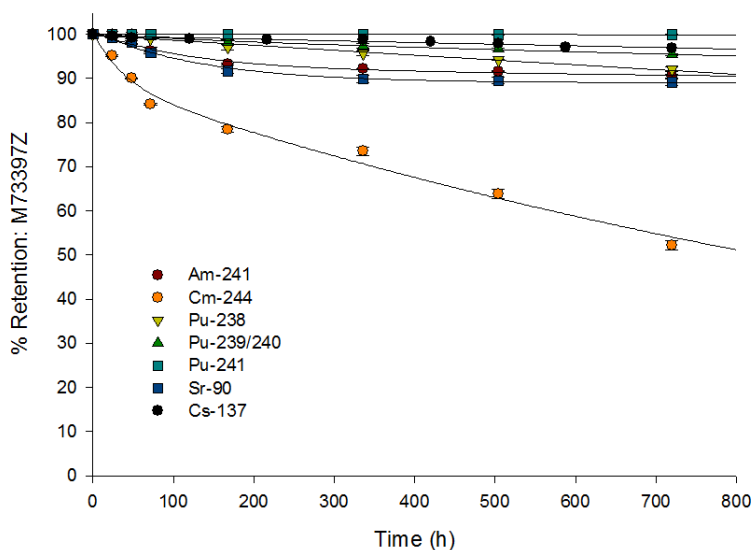
Figure 33 Individual leach rate measurements for radionuclides associated with irradiated UO_2 fuel ID M73397Z.

Table 11   Characteristics by radionuclide

Nuclide	Slow Dissolution Component			Faster Dissolution Component		
	f_s	k_s (d^{-1})	$t_{1/2}$ (d)	f_r	k_r (d^{-1})	$t_{1/2}$ (d)
Sr-90	0.88	2.6E-13	2.7E+12	0.12	7.4E-03	94
Cs-137	>0.99	3.9E-05	1.8E+04	-	-	-
U-238	0.88	1.8E-05	3.8E+04	0.12	9.6E-03	72
Am-241	0.91	2.3E-05	3.0E+04	0.09	8.5E-03	82
Cm-244	0.88	6.9E-04	1.0E+03	0.12	2.7E-02	26
Pu-238	0.99	9.1E-06	7.6E+04	0.01	6.9E-03	100
Pu-239/240	0.99	5.0E-05	1.4E+04	0.01	6.3E-03	110
Pu-241	>0.99	9.9E-05	7.0E+03	-	-	-
Plutonium Isotopes*	0.99	5.3E-05	1.3E+04	0.01	6.6E-03	110

*Average of values for the various plutonium species.

The values for the faster dissolution component f_r for the various radionuclides, namely, Sr-90, U-238, Am-241 and Cm-244 were similar, i.e., approximately 0.1, whereas the faster dissolution component of plutonium isotopes was essentially zero. Excluding the k_s values for Sr-90, which was exceptionally low and Cm-244, the average k_s value for the other radionuclides was 4.2E-05 d^{-1}. Excluding the k_r values for Cm-244, the average k_r value for the other radionuclides was 7.6E-03 d^{-1}. Table 14 presents the solubility classifications for the various radionuclides present in irradiated UO_2, obtained by comparing the results with the default ICRP 66 parameters for Solubility Classification shown in Table 11. Dual classifications were identified for Sr-90, U-238 and Cm-244; the Solubility Class for the remaining radionuclides was determined to be Class S.

Table 12 Solubility Classifications for Various Radionuclides in Irradiated UO2

Radionuclide	ICRP Solubility Class
Sr-90	M based on f_r, S based on k_s
Cs-137	S
U-238	M based on f_r S based on k_s
Pu-238	S
Pu-239/40	S
Pu-241	S
Am-241	S
Cm-244	M based on f_r S based on k_s

To more definitively establish the solubility classifications for Sr-90, U-238 (irradiated) and Cm-244, their fitted values were compared with those for Class S and Class M materials as shown in Figure 34. Due to the proximity of the data for Sr-90 to that of ICRP Class S, this radionuclide was labelled to exhibit the behavior of Class S; whereby irradiated U-238 and Cm-244 was considered to exhibit Class M behavior.
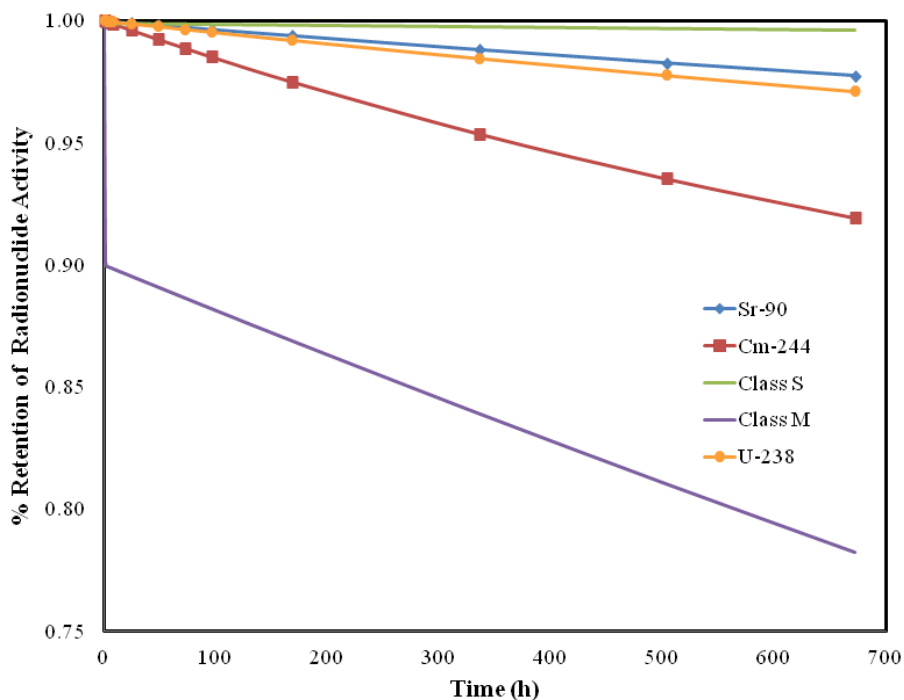
Figure 34 Percent retention of irradiated UO$_2$ fuel on filter and associated radionuclides; Sr-90, Cm-244.

Currently within Canada, the most commonly used method to identify and quantify the CED following intakes of irradiated fuel is either a semi-annual or annual urine bioassay to quantify Pu-239 intake, which is followed by dose attribution for the other associated radionuclides. It is assumed that the various actinides, fission products and other fuel constituents will 'leach' at comparable rates due to the bulk dissolution of the irradiated UO$_2$ fuel upon deposition in the lung. Again, accuracy of this approach is dependent on the assumed isotopic composition inhaled by the worker and the assumption that each radionuclide within the material matrix dissolves at the same rate. The results indicate that this is perhaps an invalid approach, as some actinides and fission products are leaching from the bulk irradiated material in the lungs at considerably faster rates. This allows for further excretion or transportation to targeted tissues/organs where residing will deliver a localized dose other than at the site of initial deposition.

7. ANIMAL STUDY: LUNG SOLUBILITY OF IRRADIATED UO$_2$ FUEL

- The Technical outline was approved February 2015.
- Scientific Merit reviewed and Animal protocol approved by the CRL Animal Care Committee (ACC) June 2015.
- Study commenced September 2015.
- The following is an overview of the study.

7.1 Scientific Rationale

In vivo studies are considered to be the gold standard when it comes to obtaining information and data on the lung solubility of airborne particulate. This study will further provide a benchmark against which the utility of the *in vitro* methods can be assessed.

Following the inhalation of airborne irradiated nuclear material/debris such as UO$_2$ fuel particulates, the actinide isotopes and fission products in the matrices of this material will be mechanically cleared, retained in the lungs or absorbed and transported by blood (absorption rate depends on the dissolution properties of the initial physic-chemical form) prior to deposition in target organs and tissues (e.g., bone, liver, kidney). There, they are retained, excreted via urine/faeces or will re-enter the blood circulation. Particular concern surrounds the retention and deposition of the actinide isotopes (e.g, Am-241, Cm-244) as they are highly radiotoxic and can lead to the induction of malignant tumours [25]. Due to their high specific activities, the radiotoxic properties of these radionuclides predominate over any possible chemical toxicity, and therefore serious radiation injury may be induced by very small masses of the element. For example, both Am-241 and Cm-244 decay by alpha-particle emission with mean energies in the range of 4.8-6.1 MeV. The relatively short half-life of Cm-244 of 18 years means that its specific activity of 3 x 10^{12} Bq/g is high. Although present in very small amounts by comparison to some other actinides, this is still 23 times higher than that of Am-241 (1.3 x 10^{11} Bq/g) and 1300 times higher than Pu-239 (2.3 x 10^9 Bq/g) [26].

Currently, bioassay (fecal or urine) sample analysis is required to verify solubility classification (insoluble (S), moderately soluble (M) or soluble (F)) for a material in order to select the proper biokinetic models according to ICRP recommendations for dose calculations following an exposure [2, 21, 27]. Therefore, it is of fundamental importance to understand the retention characteristics of irradiated fuel particulate and its associated actinide isotopes in the lungs, and the rate at which these isotopes enter the blood circulation for deposition in target tissue and organs. It is also of value to develop a realistic lung model and biokinetic data for this material, as it is needed for the assessment of the radiation doses delivered to the organs and tissues of an exposed individual. This knowledge is also an essential prerequisite for the development of safe and efficacious therapeutic methods for accelerating their slow, natural rate of elimination from the body in the event of a serious accidental contamination.

The objective of this study is to obtain much of this information with the aim of significantly narrowing the gap in knowledge, which resides in our current workplace radiological protection and dosimetry monitoring programs for such inhalation hazards. To do this, an animal study is required. The study will simulate the inhalation of irradiated UO$_2$ fuel by intratracheal

instillation and deposition of the material into the lungs. Over a designated time period and specific sacrifice end-points, tissues and organs will be harvested and analyzed to evaluate the total mass and activity of the material and its actinide isotopes, Sr-90 and Cs-137. This will allow for the generation of lung retention data, the rates at which each isotope enters the blood circulation, the rate of deposition and retention in target organs, and excretion. The outcome will be improved information on this material that was previously unknown that can be used directly for an individual's dose calculation following an accidental inhalation exposure.

7.2   Experimental overview

Experiments were performed on male Long-Evans (CRL: LE) rats weighing approximately 300 g. All rats were acclimatized to their new surroundings upon arrival for a minimum of 10 – 14 days prior to use in the study. The rats were kept under constant temperature (~23 ± 1-2 °C) with a 12 h light: 12 h dark cycle, and free access to rodent chow and water. All work with the rats is conducted within the Biological Research Facility (BRF) in accordance with the Canadian Council on Animal Care (CCAC) regulations for performing animal experiments and with an ACC approved animal protocol.

For this work, a stock suspension of irradiated UO_2 fuel, 1-5 µm sized particles, in a suspension of BLES® bovine lung surfactant, was prepared for all *in vivo* administrations. All solutions for delivery to lungs, gastrointestinal (GI) tract and intravenously were prepared under sterile conditions or procedures such that they all contain a physiological pH of ~7.2-7.4. The accuracy of delivering the solution (dose) to the animals by intratracheal instillation, oral gavage and intravenous injection was evaluated by pre- and post-weighing of the syringe and catheters. The intratracheal instillation and oral administration of the stock fuel solution to the animals requires the use of a 1 ml syringe with an attached catheter and a feeding tube, respectively. The use of BLES® (bovine lipid extract surfactant) as the delivery vehicle for the fuel particles was chosen to prevent sample loss due to adherence to the interior surface of the syringe and catheter.

Both gavage administration of this solution and intravenous administration of the dissolved fuel particulates (as a citrate or nitrate solution) will be done in order to measure the solubility of the fuel in the GI tract and to monitor re-absorption into the GI once in the blood stream. This is an approach that is used to determine the radionuclides that are released in a soluble form within the GI tract. This can be described according to the equation below, where the fractional uptake in the GI tract (GI uptake) is equal to the fractional uptake as citrates ($M_{citrate/nitrate}$), divided by the fractional uptake in the GI tract that was administered as a suspension (M_{gavage}).

$$GI_{uptake} = \left(\frac{M_{citrate/nitrate}}{M_{gavage}} \right)$$

Table 15 shows the animal treatment groups, number of animals per group, dose/treatment to be delivered per animal, delivery methods and sacrifice end points for the study. For statistical analysis and the increased error that can occur with animal research, a total of 5 animals per treatment group were deemed necessary. The dose to be delivered to each animal (10 kBq) was chosen based on the preliminary actinide concentrations present in the stock fuel sample. Based

on literature reviews and previous animal protocols, this activity was determined to be safe and to deliver no significant early radiotoxic effects to the animals that could influence the dissolution and clearance rates.

Table 13 Animal treatment groups and end-points.

TREATMENT GROUP	# OF ANIMALS	TREATMENT (Bq/rat)	DELIVERY METHOD	EUTHANASIA (h)
CONTROL-1	5	BLES® *Lung surfactant (bovine)*	Intratracheal	24
CONTROL-G	5		Gavage	168 (1 week)
CONTROL-I.V	5		Intravenous	168 (1 week)
A- FUEL-2	5	10kBq (300 µL) in BLES®	Intratracheal	24
A- FUEL-3	5		Intratracheal	48
A-FUEL-4	5		Intratracheal	72
A-FUEL-5	5		Intratracheal	168
A-FUEL-6	5		Intratracheal	336
A-FUEL-7	5		Intratracheal	504
A-FUEL-8	5		Intratracheal	672 (1 month)
A-FUEL-9	5		Intratracheal	1344 (2 months)
A-FUEL-10	5		Intratracheal	2016 (3 months)
A-FUEL-G	5		Gavage	168 (1 week)
A-FUEL-I.V	5	10 kBq (citrate)	Intravenous	168 (1 week)
TOTAL	70			

7.3   Tissue Harvesting

At each endpoint established per treatment group, the animals are euthanized under inhalant anaesthetic and by cardiac puncture to collect the blood volume of the rat (~10 ml), followed by cervical dislocation. Established post-mortem procedures are followed for tissue collection. All samples are weighed, labelled and stored at -20°C until ready for radiochemical analysis preparation procedures. Note: Gamma spectroscopy will be performed on whole tissues for Cs-137.

7.4   Tissue Ashing & Digestion

For preparation of each tissue sample prior to radiochemical analysis, each receives the appropriate tracers/carriers for correction of any loss of chemical recovery. These additions will be performed during the thawing stage of the tissues. Next, each of these samples will be dehydrated, ashed at high temperatures (2-Thermolyne Furnaces available) to produce a fine

black ash.   The samples then underwent nitric acid (HNO_3) digestion using 8M HNO_3. The volume of 8M acid added to the samples is then evaporated (keeping sample 'wet' on a hotplate and then placing into the furnace at 475°C for a minimum of 5 h). This acid treatment is repeated until a white ash is produced, which is known to easily dissolve in 8M HNO_3. The samples were then dissolved in 8M HNO_3 to be radio-chemically separated and analyzed for the actinide isotopes, Sr-90 and again for Cs-137..

7.5   Radiochemical Separation & Instrumental Analysis

The dissolved samples are subjected to a 4-cartridge radiochemical separation procedure, originally developed at AECL by Dr. X. Dai et al., for the analysis of the actinide isotopes and Sr-90 on swipe samples [28].   This is the same procedure as previously used/discussed.

7.6   Objectives

The scientific objectives of this study:

- Define the rate at which mechanical clearance of the 'inhaled' irradiated fuel occurs.
- Measure the solubility rate of the irradiated fuel matrix / leach rate of all actinide isotopes, Sr and Cs, from the lungs.
- Define the retention characteristics of the irradiated fuel's actinide isotopes, not only in the lungs and trachea, but also in the gastrointestinal (GI) tract and whole body (excretion rate).
- Assess the dosimetric consequences following inhalation of irradiated fuel,
    - o   relative dose contributions (as a percent of total dose) from the identified isotopes
    - o   identify the actinide isoptope/s delivering highest alpha dose
- Assign the appropriate ICRP inhalation solubility class to the irradiated fuel particles.

8.   SUMMARY

- Applying Stokes equation to calculate the settling rate of materials in a water column to obtain particles of a specific size range is a fast, accurate and effective method that can be used to provide particles of different materials of a comparable size.

- The proposed radionuclide sequential extraction method provides itself as a screening tool and as a standardized means of obtaining material specific information that is necessary to allow for an improved assessment of environmental and human health risk from released radiological hazards. It demonstrated:

  - *The effect of reactor burn-up on the dissolution of UO_2 fuel, in that it provides a more 'soluble fraction' of uranium due to the structural and chemical changes exhibited during reactor operation.*

  - *The dissolution of ^{241}Am, ^{244}Cm, ^{90}Sr and ^{137}Cs being a result of the dissolution of the bulk irradiated UO_2 fuel structure.*

  - *Those plutonium isotopes exhibited a solubility profile that was found to be significantly different than all of the other radionuclides measured.*

- The flow *in vitro* dissolution of un-irradiated UO_2 demonstrated a lower calculated percent error for all replicates performed (n=3) when compared to the static *in vitro* test. The values obtained from the flow test of UO_2 solubility were deemed most accurate to reflect simulated lung solubility of un-irradiated and irradiated UO_2 fuel, as well as ThO_2:

  - *Un-irradiated UO_2: Type S, >95% dissolution at a rate <0.0001 d^{-1}*

  - *Irradiated UO_2: Type M, >10% dissolution at a rate <0.005 d^{-1}*

  - *ThO_2 demonstrated a very slow dissolution rate of <<0.0001 d^{-1}: assigned Type S.*

- Preliminary *in vivo* results of un-irradiated UO_2 and ThO_2:

  - Following tracheal instillation of the UO_2 and ThO_2 into the lungs, a significant fraction of both uranium and thorium experienced rapid clearance from the respiratory tract (lungs/trachea). 71.4% of uranium and 62.9% of the thorium cleared with a half life of 0.24 d and 0.25 d, respectively. The rapid clearance of these fractions is likely a result of the mechanical clearance

  - For the remaining uranium deposited in the lungs, 12.3% and 16.3% cleared with a $T_{1/2}$ of 59 d and 433 d, respectively. For thorium, 9.1% cleared with $T_{1/2}$ of 41 d, while the largest fraction (28%) cleared slowly with a $T_{1/2}$ of 1732 d.

- Based on work presented, burn up will significantly affects the biological solubility of UO_2 fuel following intake to the lungs.

- Following an inhalation intake of irradiated UO_2 fuel from PNGS, alpha-emitting radionuclides contribute the highest estimated dose despite both percent mass or percent activity contributions. The actinides accounted for more than 62% and as much as 85% of

the estimated CED following an inhalation. The major alpha-dose contributor was Am-241 among all five fuel samples. Significant dose contributions were also observed from Pu-238, 239, 240 and 241, Sr-90 and notably Cm-244.

- Cs-137 provides itself as the signature isotope for an irradiated fuel intake in this case, based not only on its long half-life and strong gamma emissions, but also its extensive lung retention as it will reside at the site of deposition.

- A summary of the solubility data for the materials studied are presented in Table 15.

Table 16 Summary of Solubility Data

Radionuclides	Slower Dissolution Component			Faster Dissolution Component			Solubility Class
	f_s	k_s (d^{-1})	$t_{1/2}$ (d)	f_r	k_r (d^{-1})	$t_{1/2}$ (d)	
Th (Un-irradiated ThO$_2$)	1.0	4.7E-06	1.5E+05	-	-	-	**S**
U (Un-irradiated UO$_2$) - *Static* **U** (Un-irradiated UO$_2$) - *Flow*	0.99 0.95	5.7E-05 6.9E-06	1.2E+04 1.0E+05	0.014 0.05	5.0E-02 2.6E-03	14 267	**S**
Sr-90 (Irradiated UO$_2$)	0.88	2.6E-13	2.7E+12	0.12	7.4E-03	94	**S**
Cs-137 (Irradiated UO$_2$)	>0.99	3.9E-05	1.8E+04	-	-	-	**S**
U-238 (Irradiated UO$_2$)	0.88	1.8E-05	3.8E+04	0.12	9.6E-03	72	**M**
Am-241 (Irradiated UO$_2$)	0.91	2.3E-05	3.0E+04	0.09	8.5E-03	82	**S**
Cm-244 (Irradiated UO$_2$)	0.88	6.9E-04	1.0E+03	0.12	2.7E-02	26	**M**
Pu (Irradiated UO$_2$)	0.99	5.3E-05	1.3E+04	0.01	6.6E-03	110	**S**

9.   ON-GOING WORK

The table below indicates the work remaining that will be reported on to the CNSC in 2016.

Despite best efforts, some work experienced delay. This was due to the activity levels of this work and of other higher activity work going on in parallel. Therefore, primary technologist could not proceed due to Maternity status.   Work has now reconvened as a new radiochemical technologist has joined the team.

Tasks	% Complete	Comments
1. *In vitro* Flow tests:		
Fuel M73397Z	100%	*Completed*
Fuel N58817C	98%	*Data received & being analyzed*
Fuel N40589C	98%	*Data received & being analyzed*
Fe_3O_4 debris	25%	*Work to continue April – July*
Z_rO_2 debris	10%	*Work to continue April - July*
2. *In vitro* chemical extraction:		
N58817C	90%	*Replicate (n=3) complete, Separations complete & waiting on instrumental results.*
Fe_3O_4 debris		*April- July*
Z_rO_2 debris		*April – Sept.*
3. *In vivo* Lung study: irradiated fuel	100%	*2015-11-01*
Instillations/treatments	100%	*2015-12-15*
Euthanasia/post-mortems	90%	*Current*
Ashing/tissue digestion	90%	*Current*
Radiochemical separation/analysis		

Preliminary results on the Flow dissolution of Irradiated Fuel Burn up ID's: N58817C & N40589C. Figure 36 represents the dissolution of irradiated U-238.
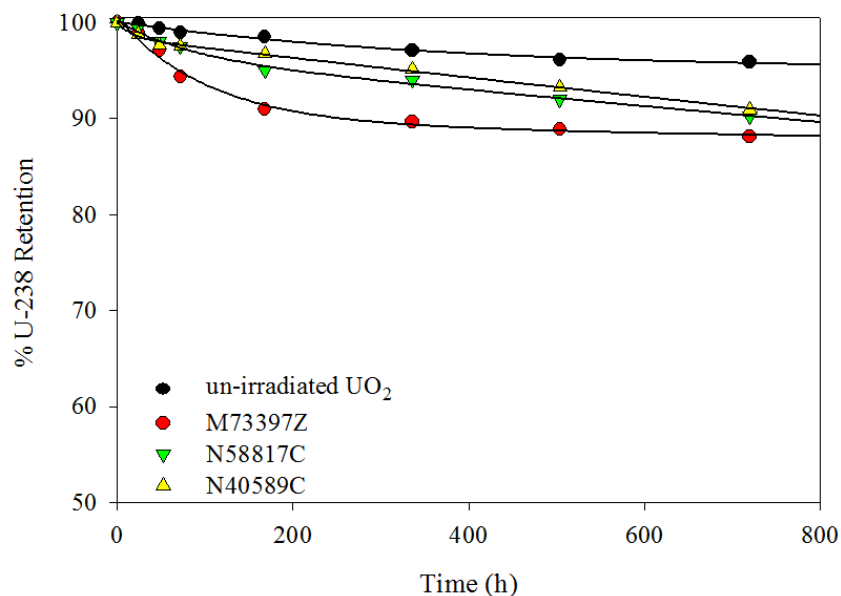
Figure 35 Results on the % dissolution of irradiated U-238 for fuel sample burn up ID's: M73397Z, N58817C and N40589C; compared with un-irradiated U-238.

Burn up ID	Residency time at discharge (d)	Burn up (MWh/kgU)	Power kW
M73397Z	582	274	588
N58817C	584	244	546
N40589C	348	157	595

- Slight variability in the % dissolution of U-238 from the irradiated fuel burn up samples.
- Plot demonstrates an increase (small) in dissolution according to burn up.

10.   REFERENCES

1.   Independent review of the exposure of workers to alpha radiation at Bruce A restart. 2011, Toronto, Canada: Radiation Safety Institute of Canada.

2.   ICRP., Human Respiratory Tract Model for Radiological Protection. Publication 66, Annals of the ICRP, 1994. **24**(1-3).

3.   E. Ansoborlo, et al., Review and Critical Analysis of Available In Vitro Dissolution Tests Health Physics, 1999. **77**(6): p. 638-645.

4.   T. Kravchik, et al., Determination of the Solubility and Size Distribution of Radioactive Aeosols in the Uranium Processing Plant at NRCN. Radiation Protection Dosimetry, 2008. **131**(4): p. 418-424.

5.   W. Li, et al., In vitro dissolution study of uranium dioxide and uranium ore with different particle sizes in simulated lung fluid. Radioanalytical and Nuclear Chemistry, 2009. **279**(1): p. 209-218.

6.   G.N. Stradling, et al., The Biological Solubility in the Rat of Plutonium Present in Mixed Plutonium-Sodium Aerosols. Health Physics, 1978. **35**: p. 229-235.

7.   G. N. Stradling and J.C. Moody, Use of animal studies for assessing intakes of inhaled actinide-bearing dusts. Journal of Radioanalytical and Nuclear Chemistry, 1995. **197**(2): p. 309-329.

8.   I. Hastings, et al., We can use thorium, in Nuclear Engineering International. 2009. p. 30-31.

9.   G. N. Stradling, et al., Thorium Nitrate and Dioxide: Exposure Limits and Assessment of Intake and Dose after Inhalation. National Radiological Protection Board, 2004: p. 1-63.

10.   D. K. Modna, et al., Thorium in the workplace measurement intercomparison. Applied Radiation and Isotopes, 2000. **53**: p. 265-271.

11.   T. T. Mercer, On the role of particle size in the dissolution of lung burdens. Health Physics, 1967. **13**: p. 1211-1221.

12.   A. Tessier, P. G. C. Campbell, and M. Bisson, Sequential extraction procedure for the speciation of particulate trace metals, in Analytical Chemistry. 1979. p. 844-851.

13.   Blanco, P., F. Vera Tomé, and J.C. Lozano, Sequential extraction for radionuclide fractionation in soil samples: A comparative study. Applied Radiation and Isotopes, 2004. **61**(2-3): p. 345-350.

14.   J. R. Duffield, et al., Handbook on the Physics and Chemistry of the Actinides. 1986, New York, USA: Elselvier Science.

15.   I. Outola, et al., Optimizing standard sequential extraction protocol with lake and ocean sediments. Journal of Radioanalytical and Nuclear Chemistry, 2009. **282**(2): p. 321-327.

16.   M. K. Schultz, et al., Identification of radionuclide partitioning in soils and sediments: Determination of optimum conditions for the exchangeable fraction of the NIST standard sequential extraction protocol. Applied Radiation and Isotopes, 1998. **49**(9-11): p. 1289-1293.

17.   M. K. Schultz, et al., New Directions for Natural-Matrix Standards - the NIST Speciation Workshop. Radioactivity and Radiochemistry, 1996. **7**(1): p. 9-12.

18.   M. Sutton and S. R. Burastero, Uranium(VI) solubility and speciation in simulated elemental human biological fluids. Chemical Research in Toxicology 2004. **17**(11): p. 1468-1480.

19.   E. Ansoborlo, et al., Review and critical analysis of available in vitro dissolution tests, in Health Physics 1999. p. 638-645.

20.   Human Respiratory Tract Model for Radiological Protection. International Commission on Radiological Protection Publication 66, 1994. **Ann. ICRP 24**(1-3).

21.   ICRP., Individual monitoring for interal exosure of workers. Annals of the ICRP, ICRP Publication 78, 1997. **27**(3-4).

22.   E. K. Garger, et al., *Solubility of airborne radioactive fule particles from the Chernobyl reactor and implication to dose.* 43, 2004(43-49).

23.   [DSPIC-508791-PRO-023], *Rapid Uranium Analysis Procedure.* 2011. **Atomic Energy of Canada Ltd.**

24.   [DSPIC-508791-PRO-026], *Rapid Thorium Analysis Procedure.* 2011. **Atomic Energy of Canada Ltd.**

25.   Taylor, D.M., *The Comparative Carcinogenicity of ^{239}Pu, ^{241}Am and ^{244}Cm in the Rat.* Proceedings of 22nd Hanford Life Sciences Symposium, Richland, WA., 1986: p. 404-412.

26.   F. Ménétrier, D. M. Taylor, and A. Comte, *The biokinetics and radiotoxicology of curium: A comparison with americium.* Applied Radiation and Isotopes, 2008. **66**(5): p. 632-647.

27.   ICRP., *The metabolism of plutonium and related elements.* Annals of the ICRP, ICRP Publication 48, 1986. **16**(2-3).

28.   X. Dai and S. Kramar-Tremblay, *Sequential Determination of Actinide Isotopes and Radiostrontium in Swipe Samples.* J. Radioanal. Nucl. Chem., 2011. **289**: p. 461-466.